NTNU
Norwegian University of
Science and Technology

Planar Docking Algorithms for Underactuated Marine Vehicles

Jon-Erik Loberg

Master of Science in Engineering Cybernetics
Submission date: June 2010
Supervisor: Thor Inge Fossen, ITK
Co-supervisor: Morten Breivik, ITK

Norwegian University of Science and Technology
Department of Engineering Cybernetics

Problem Description

1. Perform a literature study on concepts and theory relevant for planar docking operations at sea.

2. Suggest guidance algorithms for docking an underactuated AUV with an underactuated USV.

3. Suggest guidance algorithms for docking an underactuated USV with a manned mothership.

4. Evaluate the stability properties of the suggested docking algorithms.

5. Implement the developed docking algorithms in Matlab/Simulink and perform simulation studies illustrating the behavior of the considered marine docking scenarios.uggested set of criteria. Discuss your results and suggest suitable future work.

Assignment given: 11. January 2010
Supervisor: Thor Inge Fossen, ITK

Foreword

This master thesis concludes five demanding and adventures years at NTNU and Trondheim. In the last year I have been working on this ongoing subject on marine docking operations through a project report and this master thesis. Here, I owe a great amount of respect and appreciation to my supervisor Morten Breivik at NTNU. Morten Breivik has motivated and guided me through this year with great ideas and inspiration which have truly been appreciated and I show my greatest appreciations of his assistance.

I would also like to thank the employes at Maritime Robotics for giving a practical insight to a usually theoretical everyday life. At last I would express my gratitude to the my fellow students and friends throughout these five years in Trondheim, and especially Tormod Urke giving me constructive feedback through proofreading. Also in the last year I have been sharing office with Joakim Haugen, Øivind Kåre Kjerstad, Per Nord and Vetle S. Vintervold where we all have had some good times together, which surely will be remembered.

Throughout these five years in Trondheim and NTNU, I have experienced joy and happiness, together with frustrations and long hours before final exams and deadlines. Although this have been some demanding years, it have mostly been fun and exciting to learn the field of cybernetics and meeting new friends. It is therefore with a bit of sadness I close this chapter of my life and take on new one in another part of Norway. What this new chapter will tell is a mystery, so therefore I close this one with a quote from William Shakespeare's Hamlet.

> ``We know what we are, but know not what we may be.''

Jon-Erik Loberg
Trondheim, June 21, 2010

Summary

The use of *autonomously underwater vehicles* (AUVs) has a great potential in scientific mission involving underwater exploration. However a major drawback with todays AUV missions is the launch and recovery process which are usually performed manually from a manned supply ship. These manned ships have a huge daily operation cost, and because AUVs can have operation times up to 70 hours these missions become extremely costly. Since the combination of an AUV together with a manned mothership is very costly the use of AUVs are very restricted. A solution here is to replace the manned mothership with an unmanned vehicle such as a *unmanned surface vehicle* (USV). This will reduce the cost of AUV mission drastically and therefore increase the use of AUVs on scientific missions. This motivates the need for an AUV-USV docking method which is one of the two docking scenarios treated in this master thesis. Another docking method treated here is the possibility to dock a USV together with a manned mothership without human interference. A docking method that removes the human intervention will make the USV completely unmanned, since USVs today are manually docked together with a mothership or driven back to shore by a remote control.

To achieve an understanding of the field, a summary of the most relevant findings in todays literature are given. This includes the possibility to autonomously dock together an AUV with another vehicle or installation, and other related fields such as spacecraft docking and aerial refuelling. The main findings involving AUV docking, ranges from a simple fuzzy logic procedure to more advanced methods involving trajectory planning and potential field guidance. Since no extensive previous work exist on general USV docking, a short introduction is given to the most related fields, such as spacecraft docking and aerial refuelling. During air refuelling two methods are summarised which includes racetrack pattern or waypoint paths, where the receiver aircraft has two different ways of rendezvousing with the tanker, namely point parallel- or route-rendezvous.

In both docking scenarios treated here, rendezvous guidance is developed since the vehicles are assumed underactuated. The docking procedure is divided into two stages, a homing stage and a docking stage. In the homing stage only rough guidance is needed which is not the case during docking stage where requirements are much tighter on positioning to avoid collisions. In the AUV to USV homing stage the USV does all the work, but during docking stage the AUV has full responsibility, since the USV only traverses along a straight path. The USV's path is here orientated against the wind direction to minimise the sideslip effect caused due to weather disturbances. Once the USV has converged to a straight path the AUV proceeds to docking from behind the USV to finalise docking.

For the USV to mothership docking scenario, the USV has the full responsibility during the whole docking procedure. Here the USV is underactuated, and therefore the mothership will be in motion and only has to avoid sudden manoeuvres. In the homing stage the USV will manoeuvre towards a point given on the line of sight vector between the two vehicles. Once the USV reaches this point it will steer along a circle around the mothership to avoid collisions and to position itself in clear sight of the docking point. With clear sight achieved the USV will use its forward motion to converge sideways towards the docking point, such that docking can be completed.

Finally, simulations are carried out to verify the behaviour of the developed guidance laws. During these simulations two 3DOFs underactuated USV models are being used, where both vehicles only has controllability over surge speed and yaw rate. In both docking scenarios the whole docking procedure is analysed including homing and docking stage. The simulation results shows a proper docking with a satisfying approach in both scenarios. Also the mothership's velocity is examined to understand the USV's sideway approach towards the mothership.

Contents

List of Figures

List of Tables

Chapter 1

Introduction

The topic for this Master of Science (M.Sc.) thesis is marine docking operations, which mainly consists of docking together two marine vessels without human intervention. Two independent scenarios are treated, which includes the possibility to dock an *autonomous underwater vehicle* (AUV) together with a *unmanned surface vehicle* (USV) and docking a USV with a manned mothership.

1.1 Motivation

The Earth's surface is mostly covered by water, where most of this water consists of oceans. These oceans contain huge amount of resources including sealife, minerals, and hydrocarbon. Oceans also has a huge influence on the weather and continental climate, so to be able to explore and observe the oceans would be beneficial for our well-being. Ocean exploration dates back to prehistoric times when explorers started developing ships to discover new lands and for gathering food. Today ocean exploration consists of seafloor mapping, observation of various species, long time monitoring of pollution, or radiation leakage, surveillance of pipes, and other underwater installations related to the oil industry.

Many important scientific missions demand that the data is acquired during bad weather or in dangerous areas, like under the Arctic ice or around a oil leakage in deep water. In most of these cases it is to dangerous for humans, and during long time monitoring it is also to costly or boring for humans to perform the acquisition. Since humans will not perform dangerous assignments and it is too costly during long time missions, the use of unmanned vessels in dull, dangerous, and dirty missions have a great potential both economically and in the span of missions.

The use of unmanned marine vessels today consists mainly of AUVs and *remotely operated underwater vehicles* (ROVs), but lately the interest for USVs has grown. Despite of the minor interest for USVs, they have been around for some time, with the first experimentation tacking place during Word War II. Mainly development of USVs began in the 1990s with the military by developing surveillance systems and sophisticated USV mine sweeping. USVs are today being used for mapping, pollution detection, environmental surveying, and numerous other applications. USVs have the capability of much longer operating time than AUVs, and one beneficial idea would be to combine AUV technology with USV technology.

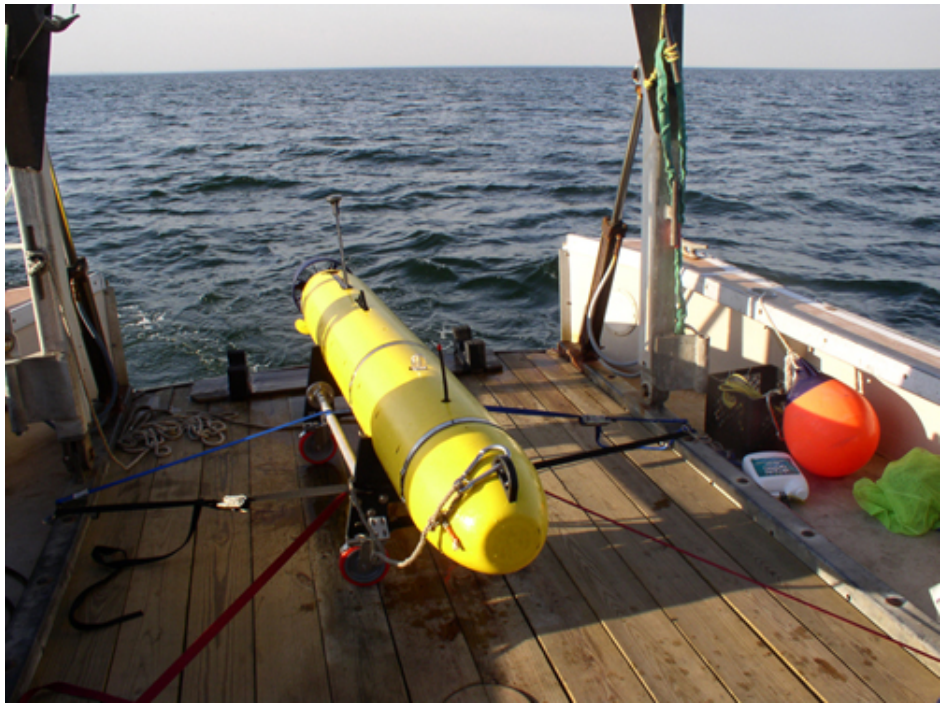

Figure 1.1: A Bluefin-12 AUV onboard its manned mothership. Courtesy of Bluefin Robotics, http://www.bluefinrobotics.com.

The use of AUVs today can be very expensive because manned ships are being used for launching and recovering AUVs. An economical issue with this method is the daily operating cost for a manned ship which usually ranges between 15.000 and 35.000 USD. AUVs today begin to get higher operational time, and especially the REMUS 600 which have an operating time up to 70 hours depending on speed and sensor configurations (Kongsberg Maritime, 2010). Recovery of an AUV starts when the AUV detects a low battery or is finished with its mission. The AUV then has to return to a mothership, which have been staying in the neighbourhood of the AUV's mission area. Since the mothership has to stay close to the AUV when its returning, it is not practical for the mothership to return to land while the AUV is surveying. Due to the operational cost of a manned mothership and the time span, the AUV missions can become extremely expensive. If AUVs are going to use their full potential, there has to be developed an affordable and productive method for deploying and recovering AUVs. Such a affordable method will open up the way for more long-term and low-budget missions using AUV technology, and more important discoveries can be made. One method that can have a huge potential is to replace the manned mothership with a USV.

Figure 1.2: The Mariner USV operating in the Trondheimsfjord. Courtesy of Maritime Robotics, http://www.maritimerobotics.no.

A method for docking an AUV with a USV would reduce the cost of AUV missions drastically and therefore have a great impact on commercial use of AUVs and research itself. With this method, researchers could have AUVs constantly out on various missions like surveillance of fish streams, seafloor mapping, and long-term monitoring of pollution. If AUVs could constantly be out on missions collecting data or samples, the amount of collected data would increase drastically.

Another method with high potential is to autonomously dock a USV with a manned mothership such that USVs can be parked onboard the ship. To autonomously dock a USV with a mothership is an untouched field of research, but the docking process is however performed today. How this is carried out today, is that the USV is remotely operated from the mothership or land. If the human interference could be removed the USVs could return to the mothership or marina without the supervision of humans, and in this case they would become completely unmanned, and therefore reduce a human stress factor.

1.2 Previous Work

Automated docking with various vehicles have been researched for many years, especially involving spacecraft. Despite many years of research in various fields, most of the docking involving aircraft and marine vessels are performed manually. The most studied field in automated marine docking is the docking of an AUV with various other vessels. The earliest docking methods here includes the docking of an AUV with a seabed mounted platform or another underwater vehicle. Lately there has been developed some methods on docking AUVs to floating platforms or another surface vehicle. Some of these methods can be adapted and fitted into an AUV - USV docking scenario and are therefore treated here.

1.2.1 Underwater AUV Docking

In the work of Rae & Smith (1992) a fuzzy rule based docking procedure is suggested, which allows an AUV to dock with another stationary underwater vehicle. The fuzzy logic controller which is suggested, drives the AUV recursively towards the final docking point. In this method there are made no assumptions about the presence, strength or direction of the currents, and the fuzzy approach does not rely on specific waypoints or high accuracy manoeuvres.

A more sophisticated method is presented in (Hong et al., 2003), where path generation algorithms are derived for docking AUVs underwater. This work divides the docking procedure into two separate stages of accuracy, a homing stage

and a docking stage. During the homing stage, distance between the AUV and the docking point is large and therefore low accuracy guidance is generated, which locates the AUV about 10 metres in front of the launcher. Since the accuracy is low during this stage the path is only generated once. This is not the case during the docking stage which is divided into two stages. In the first docking stage the paths are regenerated every given time interval, and during the final stage real-time position through visual tracking techniques is used to track the movement of the launcher, such that a successful docking can be achieved.

Another method for underwater AUV docking is presented in (Yakimenko et al., 2008). Here the AUV returns to a prearranged point when it has completed its mission. Once the AUV arrives at the prearranged meeting point, communication is established between the AUV and a *mobile underwater recovery system* (MURS) which have been waiting nearby. The MURS suggests a rendezvous point (area) and time, and then sends this information to the AUV, which then plans trajectories to rendezvous with the recovery unit, see Figure 1.3. These trajectories are then recomputed every couple of seconds, and then sent back to the recovery unit such that both vessels can execute the plan simultaneously. This work are focusing on the trajectory generation, since it is assumed that the control laws are already implemented in AUV.

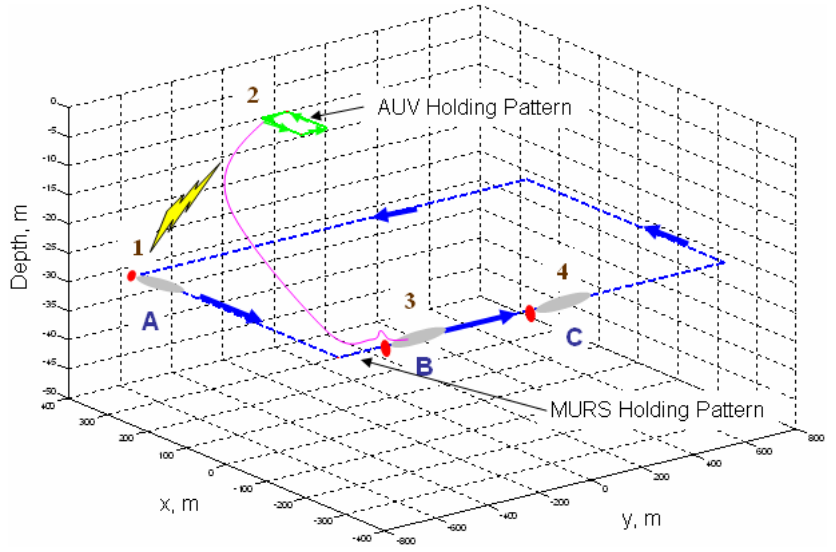

Figure 1.3: AUV and the mobile underwater recovery system in (Yakimenko et al., 2008).

1.2.2 Surface AUV Docking

In (Martins et al., 2007) a hybrid coordinated manoeuvre for docking an AUV with an *autonomous surface vehicle* (ASV) is described. The paper presents a vision-based navigation system mounted on top of the ASV for detecting a free-floating AUV, which could be without power. It is assumed that the vision system can detect the AUV on the surface and that the navigation is compact and precise such that currents could be estimated. Before an approach towards the AUV begins, a preparation phase is executed which turns the ASV towards the AUV. Once the preparation is done, the ASV approaches the AUV with *line of sight* (LOS) guidance, such that the ASV reaches a neighbourhood of the target which is a predefined radius around the AUV. In the final docking stage the ASV goes through an alignment stage to minimise the damage on propellers and fins before final docking is executed and the AUV is being mechanically locked.

Another similar approach is presented in (Dunbabin et al., 2008), where also vision-based navigation is mounted on top of an ASV to position itself towards a floating AUV. The docking procedure here is dived into two stages, where the first stage is used to move the ASV within a pre-specified radius of the target. GPS position is used during the first stage so therefore the vessels can be located further apart than in the previous method, which only used vision navigation. In the second and final stage the vision systems takes over, and the guidance used is a virtual force field with an attractive force and a repelling force. The attractive force is located in the AUVs *centre of gravity* (CG) such that ASV would be forced towards the AUV. To achieve correct orientation during the docking, two repelling forces are placed on each sides behind the AUV. This method allows a coordinated docking between an ASV and a stationary or moving AUV.

The use of artificial potential fields is also presented in (Jantapremjit & Wilson, 2008) for docking of an AUV to a platform in 2D or 3D space. This method also divides between homing and docking strategy, and during homing stage the docking target is treated as an attractive potential, while obstacles has a repulsive potential, see Figure 1.4. The docking strategy is divided into two stages, where the first stage is a preparation stage and the second stage is a final docking stage. In the first stage, the AUV tracks a path located in a valley where the minimum virtual potential force occurs. Throughout the final docking stage, the velocity is kept within a safe range such that collisions with the platform can be avoided. A sliding mode controller is introduced in this work which provide the system's stability, and is demonstrated in a simulation.

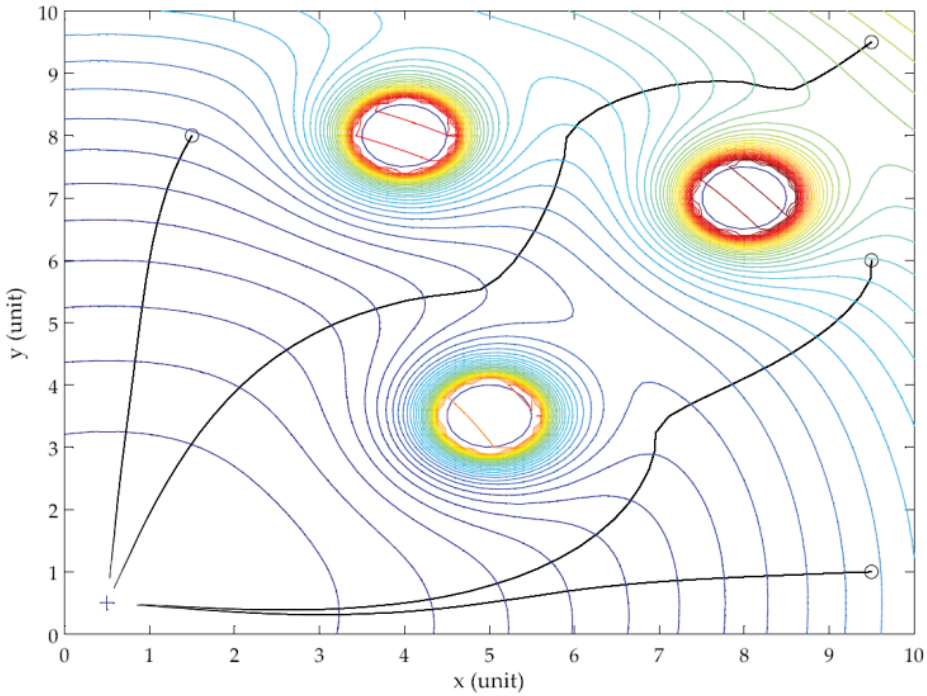

Figure 1.4: Artificial potential field with three obstacles, where ∘ defines various starting points and + defines the goal. Courtesy of Jantapremjit & Wilson (2008).

1.2.3 Docking in Various Fields

Automated docking of various vehicles is a neglected field of research since most of the docking are performed manually. However the space industry have researched automated docking for many years. Where one of the objectives with NASA's Gemini program was to dock with orbiting vehicles, and then be able to manoeuvre the vehicles afterwards. On March 16, 1966 NASA performed the first rendezvous and docking between two spacecraft when Gemini 8 docked with the RM-81 Agena. This was a manned docking, and the first automated unmanned space docking was performed by the Soviets, when they docked together Cosmos 186 and Cosmos 188 on October 30 1967 in their mission to race the Americans to the moon (Fehse, 2003).

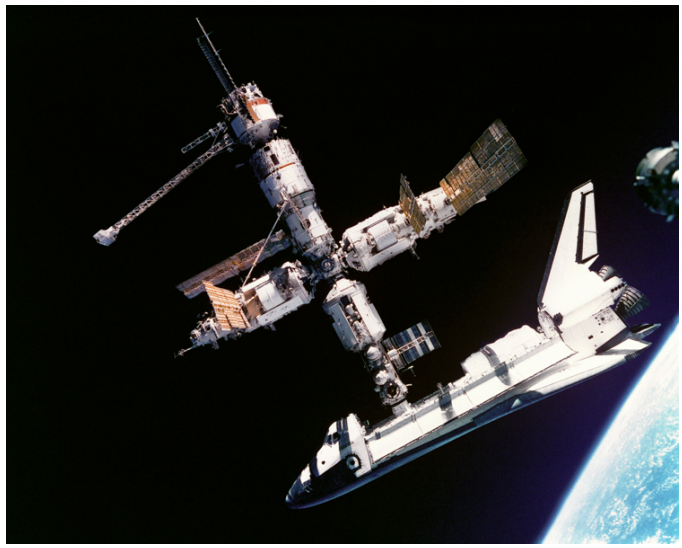

Figure 1.5: The now retired space shuttle Atlantis, docked with the Russian space station Mir on June 29, 1995. Courtesy of NASA, http://www.nasa.gov.

In spacecraft docking, both vehicles are active and are able to manoeuvre. However during the docking one craft is considered the chaser while the other one is a passive target. Here, the main goal of the passive target is to stay stable while the chaser craft executes the docking procedure (Wertz & Bell, 2003). Since the distance between the two vehicles could be immense during early stages of the docking, there is a huge responsibility on the rendezvous path planning. Here an important objective during is to use as little propellant as possible, but during final docking stage this objective changes to avoid damaging the vehicles. Once the docking is achieved the two spacecraft are mechanically locked together such that they do not uncontrollably escape from each other. A structural feature with the capture mechanism besides from locking the vehicles together is to allow some small deviations in position, attitude, and velocity.

A field which utilises a similar approach as during marine docking is the aviation industry when performing landing and air refuelling operations. The automated landing has been integrated in the aircraft autopilot for many years, and was first developed during the 1950s (The Department for Business, Innovation and Skills (BIS), 2010). Automated refuelling is a field where there has been little interest since refuelling usually concerns manned aircraft. However the interest for automated refuelling becomes interesting together with *unmanned aerial ve-*

hicles (UAVs), and the possibility to achieve longer unmanned flights. The choice of air refuelling method is related with the available air space, and is normally conducted in one of two ways: in an anchor area or along an air refuelling track (Department of Defense, 2002). In anchor areas the tanker flies a racetrack pattern within the defined airspace while waiting for the receiver aircraft to arrive. Once the receiver aircraft arrives, the tanker flies in a wider race track while refuelling the receiver. This method is best suited for small, highly manoeuvrable aircraft, and is usually conducted in friendly airspace, since it can place the tanker in a vulnerable position. The air refuelling track is a series of points, normally located along the receiver's path. The tanker can rendezvous with the receiver in two different ways: point parallel rendezvous or route rendezvous (Department of Defense, 2002). In the point parallel rendezvous, the tanker orbits a designated point along the track while waiting for the receiver to arrive, and in the route rendezvous the tanker and receiver arrange a rendezvous point where they both arrive simultaneously.

Figure 1.6: The first aerial refuelling including F-35 Lightning II stealth fighter. Courtesy of Lockheed Martin, http://www.lockheedmartin.com.

Both spacecraft docking and aircraft autopilots have lots of similarities to marine docking. It shows that an automated docking and docking procedure in general is extremely complicated and has to be well coordinated from the beginning. Without these precise and well planned guidance laws catastrophically and costly disaster could be the result.

1.3 Contributions

This master thesis explore the possibility to automatically dock together marine vessels at sea. Here, two independent docking scenarios are treated which includes the docking of an AUV together with a USV, and the potential to dock a USV with a manned mothership without human interference. The main contributions of this master thesis are summarised as

- A brief Introduction to the main findings in todays literature, including AUV docking with other vehicles and platforms, spacecraft docking and aerial refuelling.
- Introduction to the most appealing guidance laws in todays literature related to the docking of underactuated marine vessels. The two cases treated here are target tracking and path tracking.
- Development and analysis of guidance laws for AUV to USV docking scenario with analytical proof of convergence. Here a two stage docking is discussed with a rough homing stage and a precise docking stage. Further a strategy for minimising environmental disturbances and collision avoidance are examined.
- Development and analysis of guidance laws for docking a USV together with a manned mothership and analytical proof of convergence. During this case a two stage docking are discussed with a rough homing stage and an accurate docking stage. A circular manoeuvre is developed to avoid collisions when the USV closes in on the mothership.
- Derived rendezvous functions which will avoid uncontrolled behaviour of the virtual targets which the marine vessels follow on their path to complete a safe docking.

Chapter 2

Preliminaries

2.1 Notation

- **Derivatives** of a function $f(\omega)$, with respect to ω are in this report denoted $f'(\omega), f''(\omega), f^{(3)}(\omega), \ldots, f^{(i)}(\omega)$.
- **Time derivatives** of $x(t)$ are denoted $\dot{x}, \ddot{x}, x^{(3)}, \ldots, x^{(i)}$.
- The **class p-norms** defined by $\|x\|_p = (|x_1|^p + \cdots + |x_n|^p)^{1/p}, \quad 1 \leq p < \infty$, where the one most used here is the 2-norm, or the Euclidian vector norm, simply denoted $|x| := \|x\|_2 = (x^T x)^{1/2}$.

2.2 Abbreviations

ASV	Autonomous Surface Vehicle
AUV	Autonomous Underwater Vehicle
CB	Constant Bearing
CG	Centre of Gravity
DOF	Degree of Freedom
LOS	Line of Sight
MURS	Mobile Underwater Recovery System
NED	North East Down
PP	Pure Pursuit
RB	Rigid Body
ROV	Remotely Operated Underwater Vehicle
UAV	Unmanned Aerial Vehicle
UGAS	Uniformly Globally Asymptotically Stable
USV	Unmanned Surface Vehicle

2.3 Nonlinear Stability Theory

Lyapunov's Stability Theorem (Khalil 2002)

Let $x = 0$ be an equilibrium point for $\dot{x} = f(x)$ and $D \subset \mathbb{R}^n$ be a domain containing $x = 0$. Let $V : D \to \mathbb{R}$ be a continuously differentiable function such that

$$V(0) = 0 \quad \text{and} \quad V(x) > 0 \in D - \{0\}. \tag{2.1}$$

The equilibrium point $x = 0$ is *stable* if

$$\dot{V}(x) \leq 0 \in D \tag{2.2}$$

and $x = 0$ is *asymptotically stable* if

$$\dot{V}(x) < 0 \in D. \tag{2.3}$$

Proof: See Khalil (2002).

Lyapunov's Direct Method (Khalil 2002)

Let $x = 0$ be an equilibrium point for $\dot{x} = f(x)$ and let $V : \mathbb{R}^n \to \mathbb{R}$ be continuously differentiable function such that

$$V(0) = 0 \quad \text{and} \quad V(x) > 0, \quad \forall\ x \neq 0. \tag{2.4}$$

The equilibrium point $x = 0$ is *globally asymptotically stable* if

$$||x|| \to \infty \Rightarrow V(x) \to \infty \tag{2.5}$$

and

$$\dot{V}(x) < 0, \quad \forall\ x \neq 0. \tag{2.6}$$

Proof: See Khalil (2002).

Chapter 3

Mathematical Modelling

When developing mathematical models, the study can be divided into two parts (Fossen, 2002; Perez, 2005):

- Kinematics
- Kinetics,

where *kinematics* describes only geometrical aspects of motion without considering forces, and *kinetics* is the analysis of the forces causing motion. This chapter introduce these fields and relates them to the docking problem.

3.1 Kinematics

In 1950, the Society of Naval Architects and Marine Engineers (SNAME) introduced a universal notation for marine vessels. Table 3.1 summarises the adopted nomenclature for the description of ship motion.

3.1.1 Reference Frames

When describing a movement of marine vessels in 6 *degrees of freedom* (DOF), 6 independent coordinates are necessary to determine the position and orientation. Three coordinates to define translations and three coordinates to define the orientation. These coordinates are defined with the use of two types of reference frames: *inertial frames* and *body-fixed frames* (Fossen, 2002; Perez, 2005). In the marine literature the following right-hand reference frames are usually considered (see Figure 3.1 and 3.2):

Table 3.1: The notation according to SNAME (1950) with vectorial definition from Fossen (2002).

$\boldsymbol{\eta}$	**Name**	$\boldsymbol{\nu}$	**Name**
x	North position	u	Surge speed
y	East position	v	Sway speed
z	Down position	w	Heave speed
ϕ	Roll angle	p	Roll rate
θ	Pitch angle	q	Pitch rate
ψ	Yaw angle	r	Yaw rate

Earth-Centred Reference Frames

ECI The *Earth-centred inertial* (ECI) frame $\{i\} = (x_i, y_i, z_i)$ is an inertial frame for terrestrial navigation. The origin o_i is located at the centre of the Earth with the z-axis pointing along the Earth's rotational axis, and the x-axis pointing towards the vernal equinox.

ECEF The *Earth-centred Earth-fixed* (ECEF) reference frame $\{e\} = (x_e, y_e, z_e)$ have the same orientation as the ECI-frame but rotates with an angular velocity, $\omega_e = 7.2921 \cdot 10^{-5}$. ECEF frames is usually used for global guidance and GPS measurements are given in this frame.

Geographic Reference Frames

NED The *North-East-Down* (NED) coordinate system $\{n\} = (x_n, y_n, z_n)$ is fixed to Earth with origin o_n. This coordinate system have the x-axis points towards true north, y-axis points towards East, and the z-axis points downwards normal to Earth's surface. NED is our everyday coordinate system and is ideal for local navigation considering flat Earth conditions. Since the final stage of the docking problem considers relative short distances the NED-frame will be an ideal inertial frame.

BODY The body-fixed reference frame $\{b\} = (x_b, y_b, z_n)$ is moving along with the vehicle while the origin o_b is fixed to the hull. The orientation of the axis are as follows: the x-axis points in forward direction, y-axis points towards starboard, and z-axis points downward. This coordinate system is used to describe linear and angular velocities, while position and orientation are described relative to the inertial frame.

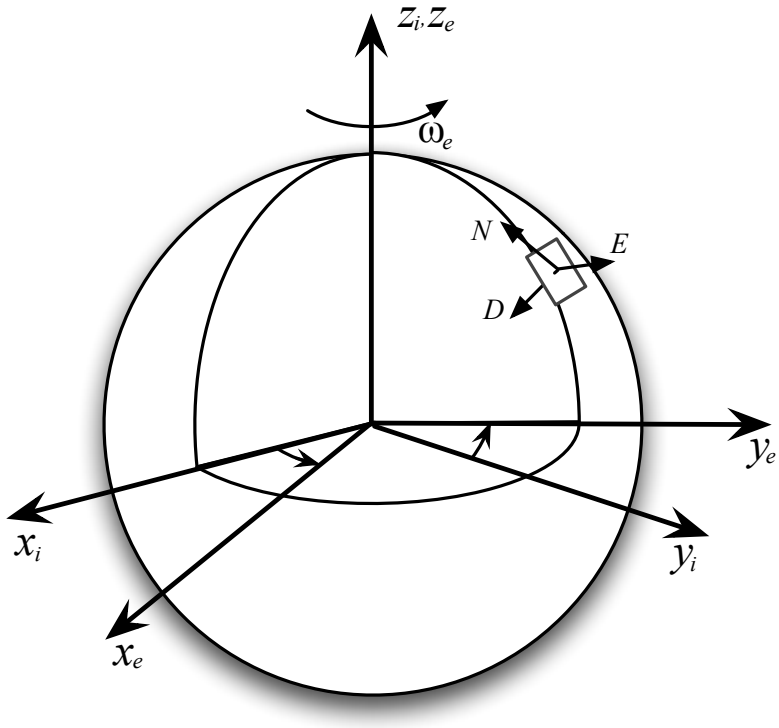

Figure 3.1: The relation between the ECI, ECEF, and NED frames.

There are numerals reference frames, especially in the field of navigation, however these are the most important considering marine vessels. In the docking problem considered here, the two geographic reference frames are of most interest, because the main problem is the final docking stage where distances are relatively short. During the initial docking stage, distances between vessels can be large, and thus requiring Earth centred reference frames in some cases.

3.1.2 Vessel Kinematics

As mentioned earlier, kinematics considers only the geometrical aspects of the vehicle. To be able to describe all the possible orientations, a 6 DOF model is needed, but since only surface docking is considered, a 3 DOF model is expressed in vector form as (Fossen, 2002):

$$\dot{\boldsymbol{\eta}} = \mathbf{R}(\psi)\boldsymbol{\nu}, \tag{3.1}$$

where

$$\mathbf{R}(\psi) = \begin{bmatrix} \cos(\psi) & -\sin(\psi) & 0 \\ \sin(\psi) & \cos(\psi) & 0 \\ 0 & 0 & 1 \end{bmatrix} \tag{3.2}$$

is the rotational matrix transforming motion from the body-fixed (BODY) frame to the inertial (NED) frame. As mentioned in Table 3.1, $\boldsymbol{\eta} = [x\,,\, y\,,\, \psi]^T$ represents the Earth-fixed position and heading, while $\boldsymbol{\nu} = [u\,,\, v\,,\, r]^T$ represents the body-fixed linear and angular velocities.

The rotation matrices belongs to a group of orthogonal matrices and therefore satisfies:

$$\mathbf{R}\mathbf{R}^T = \mathbf{R}^T\mathbf{R}, \quad \det(\mathbf{R}) = 1, \tag{3.3}$$

which implies that $\mathbf{R}^{-1} = \mathbf{R}^T$. These are very important properties of the rotation matrices and makes computation much easier.

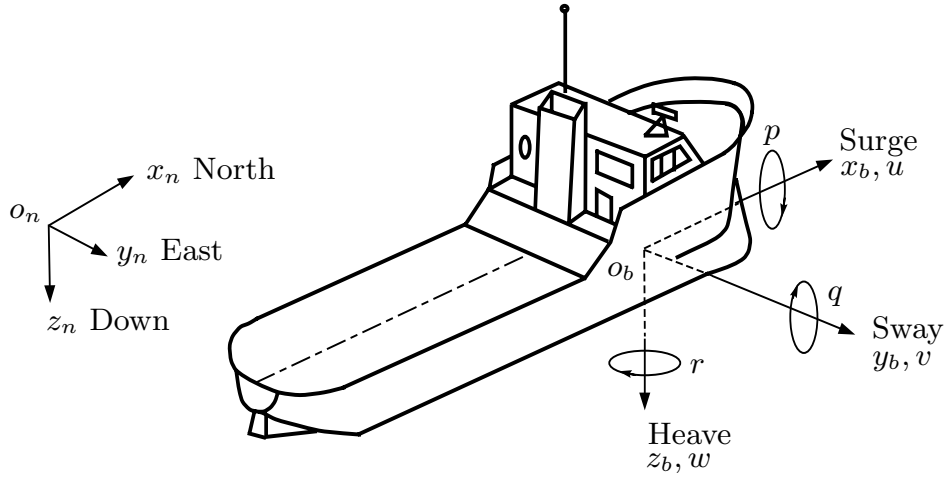

Figure 3.2: Notation and reference frames for a marine vehicle. Courtesy of Perez (2005).

3.2 Kinetics

The vessel kinetics describes the resulting motion due to forces acting on the vehicle, and involve the study of *statics* and *dynamics*. Statics concerns bodies at rest or moving with constant velocity and includes gravitational and buoyancy forces, while dynamics is concerned with bodies having accelerated motion. Many dynamic systems including marine vessels can be described as a *mass-damper-spring* system. A body of certain mass is forced into an oscillated motion with restoring forces that drives the system back into an equilibrium state. The dynamics given here is according to Fossen (2002), and have strong similarities to a mass-damper-spring system.

3.2.1 Vessel Dynamics

Since surface docking is considered, the 3 DOF horizontal dynamics is needed which neglects the vertical-working restoring forces. A vectorial 3 DOF model is according to Fossen (2002) and given by:

$$\mathbf{M}\dot{\boldsymbol{\nu}} + \mathbf{C}(\boldsymbol{\nu})\boldsymbol{\nu} + \mathbf{D}(\boldsymbol{\nu})\boldsymbol{\nu} = \boldsymbol{\tau}, \tag{3.4}$$

where each term represents:

$\mathbf{M} = \mathbf{M}_{RB} + \mathbf{M}_A$ is the system inertia matrix, including rigid-body mass matrix (RB) and added-mass matrix (A). For operating at low speeds, $\mathbf{M} \in \mathbb{R}^{3\times3}$ can be shown to be symmetrical and positive definite, i.e. $\mathbf{M} = \mathbf{M}^T$ and $\dot{\mathbf{M}} = \mathbf{0}$.

$\mathbf{C}(\boldsymbol{\nu}) = \mathbf{C}_{RB}(\boldsymbol{\nu}) + \mathbf{C}_A(\boldsymbol{\nu})$ is the Coriolis-centripetal matrix including rigid-body and added-mass effects. Effects from this term comes from rotational motions and can be neglected for straight-line motion. An important property is that $\mathbf{C}(\boldsymbol{\nu}) \in \mathbb{R}^{3\times3}$ is skew-symmetric, i.e. $\mathbf{C}(\boldsymbol{\nu}) = -\mathbf{C}^T(\boldsymbol{\nu})$.

$\mathbf{D}(\boldsymbol{\nu}) = \mathbf{D}_L + \mathbf{D}_N(\boldsymbol{\nu})$ is a matrix describing the hydrodynamic damping and is divided into a linear and a non-linear part, $\mathbf{D}(\boldsymbol{\nu}) \in \mathbb{R}^{3\times3}$. There are several causes to damping forces including potential damping, skin friction, wave drift, and vortex shedding.

$\boldsymbol{\tau} = \boldsymbol{\tau}_{thr} + \boldsymbol{\tau}_{env}$ describes external forces including propulsion and environment forces. The propulsion forces $\boldsymbol{\tau}_{thr} \in \mathbb{R}^3$ contains control inputs including propellers, thrusters, rudders, and water jets. The environment forces $\boldsymbol{\tau}_{env} \in \mathbb{R}^3$ includes mainly wind loads, 1st and 2nd-order wave loads and currents.

Chapter 4

Guidance Laws

In a docking scenario, the docking vehicle needs to be guided towards a precise position located at a docking station to achieve a successful docking. To obtain this, proper guidance laws ensures that the docking vehicle approaches the docking station in an acceptable manner. Guidance laws are typically equivalent to kinematic controllers which considers the geometrical aspects of motion, without reference to forces and moments. When considering motion of a vehicle it is useful to distinguish between two types of operation spaces, namely *work space* and *configuration space* (Spong et al., 2006). The work space represents the physical space which the vehicle moves. This contains a 2-dimensional work space for planar motion such as a USV, while a 3-dimensional work space for spatial position such as an AUV. The configuration space is the set of variables sufficient to specify the location of every point on a rigid-body vehicle.

The actuation of a vehicle is related with the degrees of freedom that are associated with the motion. In the literature it is mainly distinguished between two different actuation properties (Breivik et al., 2008), namely

- Full actuation
- Underactuation.

When the controllable DOFs equals the total DOFs, the vehicle is said to be fully actuated, because it is able to independently control all of its DOFs. This is not the case for an underactuated vehicle which has less controllable DOFs than total DOFs. Thus, an underactuated vehicle is generally unable to achieve arbitrary tasks in the configuration space, but can still be able to perform meaningful tasks in the work space.

Motion control scenarios are typically divided into the following categories: *point stabilisation*, *trajectory tracking*, and *path following*. These scenarios are given as configuration-space tasks and are best suited for fully actuated vehicles. In (Breivik & Fossen, 2009), motion control objectives are given as work-space tasks which suites underactuated vehicles better, and are defined in the following: *target tracking*, *path following*, *path tracking*, and *path manoeuvring*. Target tracking and path tracking are the two schemes that is relevant for the docking problem, path following and path manoeuvring are not, and therefore will not be discussed further in this report.

4.1 Target Tracking

The objective in a target tracking scenario is to track the motion of a target that is either stationary or moves such that the instantaneous motion is known, meaning no information about the target's future motion is available. The interceptor is represented by its planar position $\mathbf{p}(t) \triangleq [x(t)\,,\, y(t)]^T \in \mathbb{R}^2$ and velocity $\mathbf{v}(t) \triangleq \mathrm{d}\mathbf{p}(t)/\mathrm{d}t = \dot{\mathbf{p}} \in \mathbb{R}^2$, stated relative to an inertial reference frame. Defining a kinematic target and its position by $\mathbf{p}_\mathrm{t}(t) \triangleq [x_\mathrm{t}(t)\,,\, y_\mathrm{t}(t)]^T \in \mathbb{R}^2$ and velocity $\mathbf{v}_\mathrm{t}(t) \triangleq \mathrm{d}\mathbf{p}_\mathrm{t}(t)/\mathrm{d}t = \dot{\mathbf{p}}_\mathrm{t} \in \mathbb{R}^2$, the control objective of a target-tracking scenario is then stated according to Breivik et al. (2008) as

$$\lim_{t\to\infty} \tilde{\mathbf{p}}(t) = 0, \tag{4.1}$$

where $\tilde{\mathbf{p}}(t) \triangleq \mathbf{p}_\mathrm{t}(t) - \mathbf{p}(t)$ is the interceptor-target line of sight vector.

4.1.1 Pure Pursuit Guidance

Pure pursuit (PP) guidance is a two-point guidance scheme which involves the target and the interceptor. The interceptor's objective in PP guidance is to align its velocity vector along the line of sight between the interceptor and the target, as illustrated in Figure 4.1. This strategy usually results in a tail chase when the target changes position and is therefore most suitable for passive targets with zero velocity.

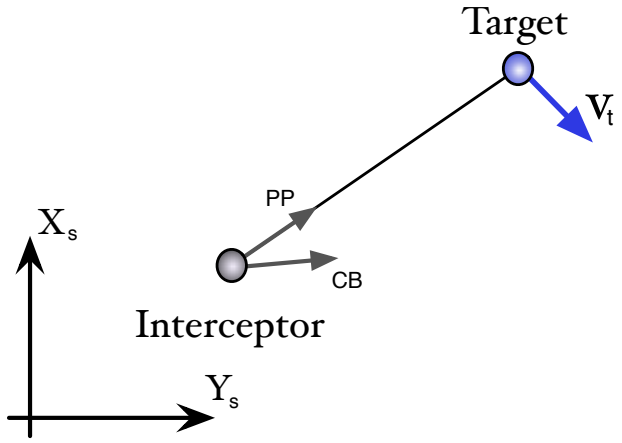

Figure 4.1: Two classical guidance principles pure pursuit (PP) and constant bearing (CB), Adapted from Breivik & Fossen (2009).

4.1.2 Constant Bearing Guidance

Constant bearing (CB) guidance is also a two point guidance scheme which involves the target and the interceptor, and is illustrated in Figure 4.1. In this case the interceptor is supposed to align the relative interceptor-target velocity along the line of sight vector between the target and the interceptor. The difference from PP guidance is that the interceptor will now reduce the LOS rotation rate to zero, which results in that the interceptor will approach the target on a direct collision course. CB guidance can be implemented through a direct velocity assignment, which means assigning a relative approach velocity along the interceptor-target line of sight vector, together with the target velocity. This is illustrated in Figure 4.2a and given according to Breivik et al. (2008) as

$$\mathbf{v}(t) = \mathbf{v}_{\mathrm{t}}(t) + \mathbf{v}_{\mathrm{a}}(t), \tag{4.2}$$

where $\mathbf{v}_{\mathrm{t}}(t)$ is the target's velocity and $\mathbf{v}_{\mathrm{a}}(t)$ is the interceptor's approach velocity towards the target, chosen as

$$\mathbf{v}_{\mathrm{a}}(t) = U_{\mathrm{a,max}}(t) \frac{\tilde{\mathbf{p}}(t)}{\sqrt{\tilde{\mathbf{p}}(t)^T \tilde{\mathbf{p}}(t) + \Delta_{\tilde{\mathbf{p}}}^2}}, \tag{4.3}$$

where $\tilde{\mathbf{p}}(t)$ is the interceptor-target line of sight vector, $U_{\mathrm{a,max}}(t) > 0$ specifies the maximum approach speed towards the target, and $\Delta_{\tilde{\mathbf{p}}} > 0$ influences the transient interceptor-target behaviour. The choice of $\Delta_{\tilde{\mathbf{p}}}$ becomes essential, because this

parameter shapes the speed transient between pursuit and rendezvous, see Figure 4.2b. A sharp velocity profile is achieved with a small value, and a soft velocity profile is achieved with a large value.

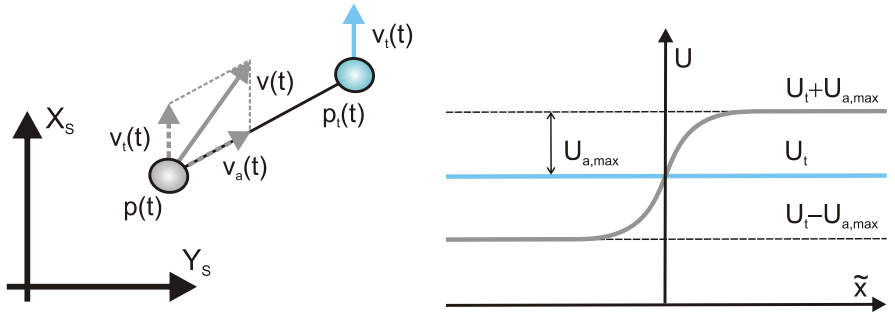

(a) (b)

Figure 4.2: Constant bearing (CB) guidance. (a) Direct velocity assignment. (b) Speed assignment along the x-axis. Courtesy of Breivik et al. (2008).

4.2 Path Tracking

The objective in path tracking is to track a target that moves along a predefined path, which is analogous to trajectory tracking. Disregarding any apriori path information this becomes a pure target tracking scenario. In this section a parametrized path and a speed law is defined, such that a virtual target can move along a predefined path.

4.2.1 Path Parameterization

A continuously parameterized planar path is achieved with assigning a scalar variable $\varpi \in \mathbb{R}$, such that position along the path is represented by $\mathbf{p}_{\mathrm{p}}(\varpi) \triangleq [x_{\mathrm{p}}\,,\, y_{\mathrm{p}}]^T \in \mathbb{R}^2$. Hence, a planar straight path is parameterized according to (Breivik & Fossen, 2009), and given as

$$x_{\mathrm{p}}(\varpi) = x_{\mathrm{f}} + \varpi \cos\alpha \tag{4.4}$$

$$y_{\mathrm{p}}(\varpi) = y_{\mathrm{f}} + \varpi \cos\alpha, \tag{4.5}$$

where $\mathbf{p}_{\mathrm{f}} \triangleq [x_{\mathrm{f}}\,,\, y_{\mathrm{f}}]^T \in \mathbb{R}^2$ represent a fixed point on the parameterizated path and $\alpha \in [-\pi\,,\, \pi]$ represent the angle of the path relative to the x-axis in an inertial frame, see Figure 4.3.

4.2.2 Target Movement

Since the objective in path tracking is to track a target that moves along a predefined path, a virtual target has to be defined and constrained to the path. Denoting the path-parameterization variable associated with the target by $\varpi_{\mathrm{t}}(t) \in \mathbb{R}$, and $\varpi_{\mathrm{t}}(t)$ can be updated according to (Breivik & Fossen, 2009) as

$$\dot{\varpi}_{\mathrm{t}} = \frac{U_{\mathrm{t}}(t)}{\sqrt{x'_{\mathrm{p}}(\varpi_{\mathrm{t}})^2 + y'_{\mathrm{p}}(\varpi_{\mathrm{t}})^2}}, \tag{4.6}$$

where $U_{\mathrm{t}} > 0$ is the speed profile with which the target traverses the path. When implementing the speed law, an initial value $\varpi_{\mathrm{t}}(0)$ have to be assigned, which defines the starting point on the parameterized path.

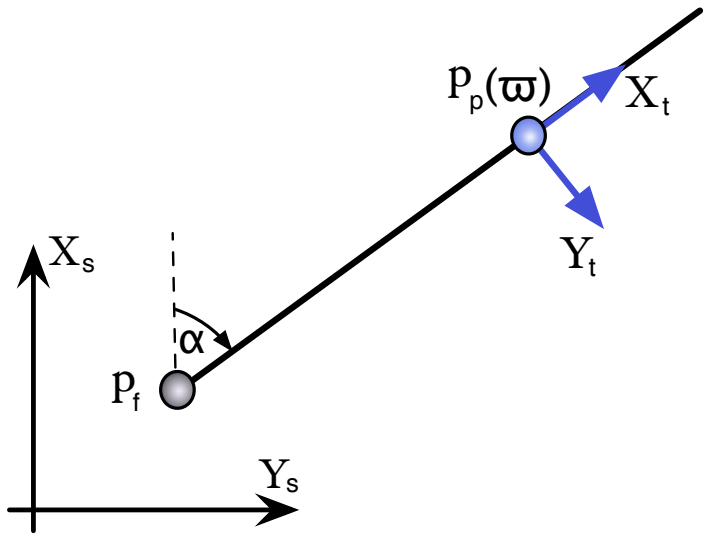

Figure 4.3: A planar straight line parameterized by a scalar variable ϖ and an arbitrary point on the path is given as $\mathbf{p}_p(\varpi)$.

Chapter 5

Docking Algorithms

Two independent docking scenarios are treated in this chapter, which includes the possibility to dock an AUV together with a USV, and the possibility to dock a USV with a manned mothership. Throughout both docking tasks the vehicles are assumed underactuated, and therefore stationary target docking cannot be performed, because underactuated vehicles have difficulties to compensate for environmental disturbances and could be forced out of position. Since docking with stationary targets are a poor strategy, both vessels will be active and in motion during the final stage of the docking scenarios, which results in the use of rendezvous docking strategy.

This chapter focuses on development of guidance laws to correctly align the vessels relative to each other to obtain a best possible docking. The guidance laws will arrange the orientation and relative speed between the two vehicles. Without a well planned strategy here the result could be crucial because collision could occur which will damage both vehicles.

5.1 AUV to USV Docking

The first docking scenario which are treated here is the possibility to dock an AUV together with a USV, and therefore increase the AUV's operational time. In the initial phase of this docking procedure, the relative distance between the two vessels can be very large. For this reason the docking scenario is divided into two stages, a homing stage and a docking stage. The main objective in the homing stage is to properly align the USV relative to the AUV, such that the docking stage has best possible initial conditions. Throughout the homing stage only rough positioning is necessary which is not the case during docking stage,

where requirements are much tighter on positioning.

In the docking stage the AUV will approach the USV from behind, before a final and proper docking is achieved. To realise a successful docking the AUV has to enter the docking station with a correct heading, such that structural damages to both vessels are avoided. Since environmental disturbances will influence the entrance heading, the USV will steer towards the disturbances such that the effect would be minimised. There are various environmental disturbances which affects the sideslip of marine vessels, but it is mainly caused by currents and waves. It is a difficult task to measure the direction of the currents and waves onboard the vessel, so in this report it is assumed a fully developed sea, meaning the waves follows the direction of the wind, which is much easier to measure. Therefore the docking path in this section is aligned against the wind direction to minimise the sideslip caused by the environmental disturbances.

5.1.1 Homing Stage

Through the homing stage the AUV will stay passive in the water such that the USV must do all the traveling. The reason for this is that the USV has much higher speed abilities and larger range than the AUV, and can therefore travel faster over greater distances. The first action in this stage is that the USV receives a docking request from an AUV, which then immediately begins to move towards the AUV's position using pure pursuit guidance scheme[1]. When the USV reaches a boundary circle which marks a predefined homing length which is illustrated in Figure 5.1, it will abandon the AUV-tracking routine. The new tracking routine will be to traverse along a straight parametrizated path[2]. The orientation of this path will be aligned against the wind direction to minimised the sideslip factor.

Two parameters are needed to realise a unique straight path, an angle and a fixed point. The angle is chosen against the direction of the wind, and the fixed point is chosen according to the USV's entrance angle γ into the boundary circle which is given as

$$\gamma \triangleq \chi_{\text{USV}}(t) - \alpha_{\text{w}}, \tag{5.1}$$

where $\chi_{\text{USV}}(t)$ is the direction of the USV's velocity, and α_{w} is the direction against the wind, i.e. $\alpha_{\text{w}} \triangleq \alpha_{\text{wind}} + \pi$. To avoid collisions between the vessels, three parallel paths are defined and the path to follow is given by the fixed point which is chosen depending on the USV's quadrant of entrance into the switching zone, and can be summarised in Table 5.1 and illustrated in Figure 5.1.

[1] Pure pursuit guidance is described in Section 4.1

[2] Straight parametrizated path is explained in Section 4.2

Table 5.1: Entrance criteria for selecting the fixed point on the USVs path.

Fixed point	Entrance angle	Quadrant
$\mathbf{p}_{f,1}$	$\lvert\gamma\rvert < 90°$ and $\gamma < 0$	1
$\mathbf{p}_{f,2}$	$\lvert\gamma\rvert \geq 90°$	3, 4
$\mathbf{p}_{f,3}$	$\lvert\gamma\rvert < 90°$ and $\gamma \geq 0$	2

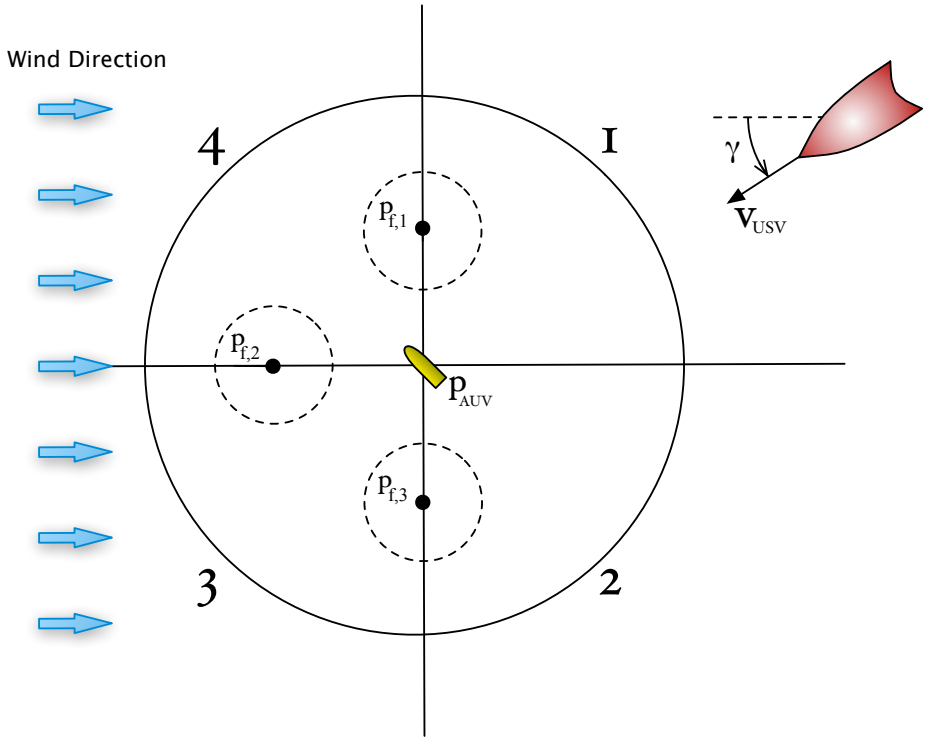

Figure 5.1: Illustration of the AUV to USV homing stage with the switch zone marked with a solid circle and activation zone for the AUV noted with dotted circles.

5.1.2 Docking Stage

In the docking stage there are much higher accuracy of the position on both vessels, and therefore more advanced guidance laws must be developed. Here the docking stage is divided into two parts, where in the first part the USV begins to track a target $\mathbf{p}_{t,USV}$ while the AUV stays passive, and the second part starts when the USV enters the dotted circle which then activates the AUV, see Figure 5.2. The dotted circle in this figure corresponds to the dotted circle in the illustration of the homing stage in Figure 5.1. Once the AUV has been activated it has the full responsibility for the docking process, since the USV will only follow a straight path without any drastic manoeuvres.

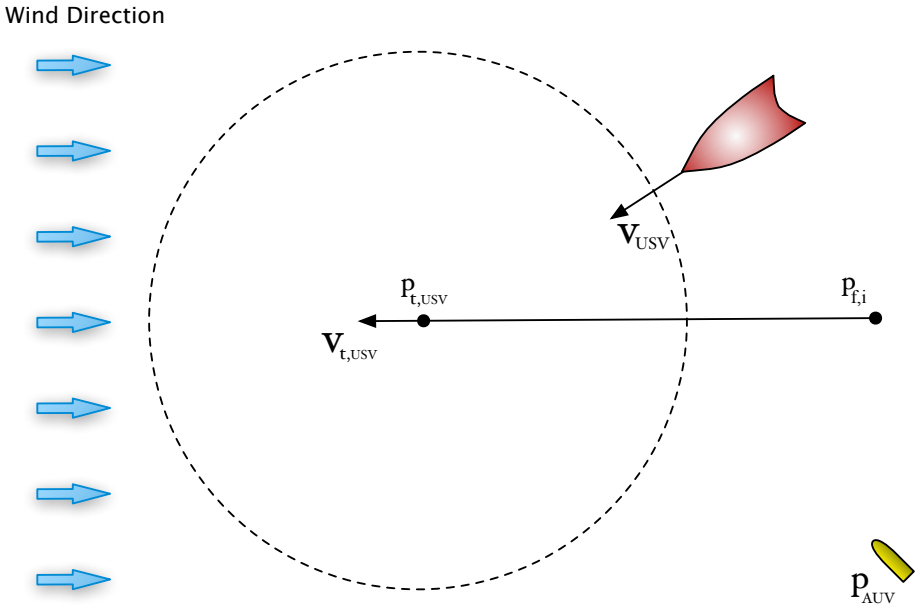

Figure 5.2: The USV tracks $\mathbf{p}_{t,USV}(t)$ while the AUV stays passive.

The USV has to follow a straight path and this is accomplished with a tracking of the virtual target point $\mathbf{p}_{\mathrm{t,USV}}$ through the CB guidance scheme[3]. The virtual target is given by

$$\mathbf{p}_{\mathrm{t,USV}}(\varpi_{\mathrm{t,USV}}) = \mathbf{p}_{\mathrm{f,i}} + \varpi_{\mathrm{t,USV}} \begin{bmatrix} \cos(\alpha_{\mathrm{w}}) \\ \sin(\alpha_{\mathrm{w}}) \end{bmatrix}, \tag{5.2}$$

where α_{w} is the direction against the wind, $\mathbf{p}_{\mathrm{f,i}}$ is a fixed point on the parameterized path, and the scalar variable $\varpi_{\mathrm{t,USV}}$ is updated through a target movement law given as

$$\dot{\varpi}_{\mathrm{t,USV}} = \frac{\mathrm{U}_{\mathrm{t,USV}}}{\sqrt{x'_{\mathrm{p}}(\varpi_{\mathrm{t,USV}})^2 + y'_{\mathrm{p}}(\varpi_{\mathrm{t,USV}})^2}}, \tag{5.3}$$

where $\mathrm{U}_{\mathrm{t,USV}} > 0$ is the speed with which the USV traverses along the path and can be noted as the constant docking speed.

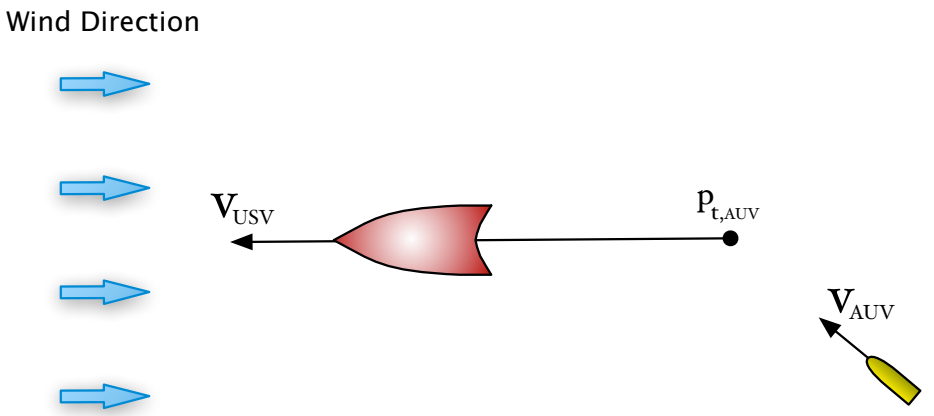

Figure 5.3: The USV has reached its tracking point $\mathbf{p}_{\mathrm{t,USV}}(t)$, such that the AUV is active and then ready to track the virtual target $\mathbf{p}_{\mathrm{t,AUV}}(t)$.

[3]CB guidance is described in Section 4.1

Once the AUV has been activated it starts to track the virtual target $\mathbf{p}_{\mathrm{t,AUV}}$, which is illustrated in Figure 5.3. This AUV target point is chosen relative to the USV and is calculated by

$$\mathbf{p}_{\mathrm{t,AUV}}(\varpi_{\mathrm{t,AUV}}) = \mathbf{p}_{\mathrm{d}}(t) + \varpi_{\mathrm{t,AUV}} \begin{bmatrix} \cos(\psi_{\mathrm{USV}}(t)) \\ \sin(\psi_{\mathrm{USV}}(t)) \end{bmatrix}, \tag{5.4}$$

where $\mathbf{p}_{\mathrm{d}}(t)$ is the given docking point and is defined as

$$\mathbf{p}_{\mathrm{d}}(t) = \mathbf{p}_{\mathrm{USV}}(t) + l_{\mathrm{d}} \begin{bmatrix} \cos(\psi_{\mathrm{USV}}(t) + \alpha_{\mathrm{d}}) \\ \sin(\psi_{\mathrm{USV}}(t) + \alpha_{\mathrm{d}}) \end{bmatrix}. \tag{5.5}$$

Here $\mathbf{p}_{\mathrm{USV}}(t)$ is the USV's position, $\psi_{\mathrm{USV}}(t)$ is the USV's heading angle, α_{d} is a fixed angle which specifies the orientation of the docking point relative to the USV, and l_{d} is the length from the USV's steering point to the docking point. These constants which defines the docking station relative to the USV is illustrated in Figure 5.4 with two different orientations. The docking point $\mathbf{p}_{\mathrm{d}}(t)$ can be located in an arbitrary distance and angle relative to the USV, and the approach path for the target point is therefore identical to the USV's heading. This will force a correct approach of the virtual target $\mathbf{p}_{\mathrm{t,AUV}}(\varpi_{\mathrm{t,AUV}})$ regardless of the USV's sideslip and heading along the path.

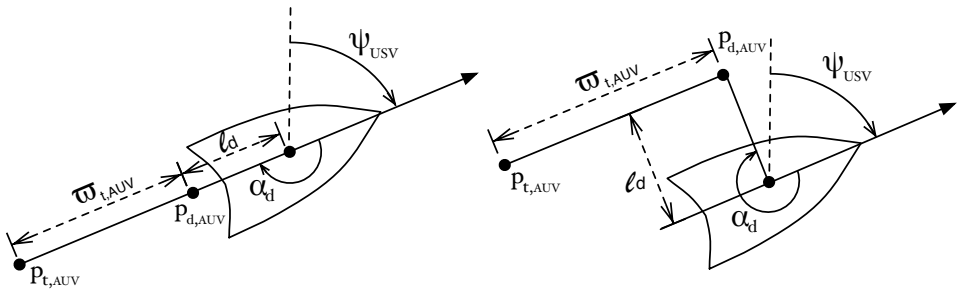

Figure 5.4: An illustration of the placement of the AUV docking point relative to the USV, (a) shows aft placement, (b) shows port placement.

The approach speed of the AUV towards the docking point is decided by the scalar variable $\varpi_{\mathrm{t,AUV}}$, which is updated by the given target movement law

$$\dot{\varpi}_{\mathrm{t,AUV}} = \frac{\mathrm{U}_{\mathrm{t,a}}(t)}{\sqrt{x'_{\mathrm{p}}(\varpi_{\mathrm{t,AUV}})^2 + y'_{\mathrm{p}}(\varpi_{\mathrm{t,AUV}})^2}}, \tag{5.6}$$

where $\mathrm{U}_{\mathrm{t,a}}(t) > 0$ specifies the approach speed towards the docking point $\mathbf{p}_{\mathrm{t,AUV}}$, and is given as

$$\mathrm{U}_{\mathrm{t,a}}(t) = \mathrm{U}_{\mathrm{t,a,max}}\rho(t)\frac{\tilde{\varpi}_{\mathrm{t}}}{\sqrt{\tilde{\varpi}_{\mathrm{t}}^2 + \Delta_{\tilde{\varpi}_{\mathrm{t}}}^2}}, \tag{5.7}$$

where $\mathrm{U}_{\mathrm{t,a,max}} > 0$ specifies the maximum approach speed, $\rho(t)$ is a rendezvous variable (see below), and $\tilde{\varpi} \triangleq \varpi_{\mathrm{d}} - \varpi_{\mathrm{t,AUV}}$ is the scalar difference between the virtual target and the docking point, for the docking point located at $\mathbf{p}_{\mathrm{d,AUV}}$ the constant ϖ_{d} equals zero (i.e. $\varpi_{\mathrm{d}} = 0$). The tuning of the function $\mathrm{U}_{\mathrm{t,a}}(t)$ is crucial in the docking controller, because this function decides the approach behaviour during the final docking stage. A too aggressive choice of parameters, i.e. large value on $\mathrm{U}_{\mathrm{t,a,max}}$ and small value on $\Delta_{\tilde{\varpi}_{\mathrm{t}}}$ will result in a fast approach which could damage both the vehicles. However a too soft tuning, i.e. small value in $\mathrm{U}_{\mathrm{t,a,max}}$ and large value on $\Delta_{\tilde{\varpi}_{\mathrm{t}}}$ will result in a slow approach, which will be time consuming and also space demanding because the vessels will cover a larger area.

The rendezvous variable $\rho(t) \triangleq \rho_{\mathrm{USV}}(t)\rho_{\mathrm{AUV}}(t)$ is introduces such that the virtual target $\mathbf{p}_{\mathrm{t,AUV}}(t)$ does not approach $\mathbf{p}_{\mathrm{t,USV}}(t)$ before the vessels tracks their individual targets properly, and are given as

$$\rho_{\mathrm{USV}}(t) = \left(1 - \frac{|\tilde{\mathbf{p}}_{\mathrm{t,USV}}(t)|}{\sqrt{\tilde{\mathbf{p}}_{\mathrm{t,USV}}^T(t)\tilde{\mathbf{p}}_{\mathrm{t,USV}}(t) + \Delta_{\tilde{\mathbf{p}}_{\mathrm{t,USV}}}^2}}\right) \tag{5.8}$$

$$\rho_{\mathrm{AUV}}(t) = \left(1 - \frac{|\tilde{\mathbf{p}}_{\mathrm{t,AUV}}(t)|}{\sqrt{\tilde{\mathbf{p}}_{\mathrm{t,AUV}}^T(t)\tilde{\mathbf{p}}_{\mathrm{t,AUV}}(t) + \Delta_{\tilde{\mathbf{p}}_{\mathrm{t,AUV}}}^2}}\right), \tag{5.9}$$

where

$$\tilde{\mathbf{p}}_{\mathrm{t,USV}}(t) \triangleq \mathbf{p}_{\mathrm{t,USV}}(t) - \mathbf{p}_{\mathrm{USV}}(t) \tag{5.10}$$

$$\tilde{\mathbf{p}}_{\mathrm{t,AUV}}(t) \triangleq \mathbf{p}_{\mathrm{t,AUV}}(t) - \mathbf{p}_{\mathrm{AUV}}(t) \tag{5.11}$$

is the line of sight vector between the USV, AUV and their respective targets.

These rendezvous variables are introduced to prevent an uncontrolled convergence of $\varpi_{\mathrm{t,AUV}}$, because large line of sight vectors on the USV or AUV will imply that $\rho_{\mathrm{USV}}(t) \approx 0$ or $\rho_{\mathrm{AUV}}(t) \approx 0$ respectively. The AUV and the USV needs therefore to track their respective targets properly before an approach of $\mathbf{p}_{\mathrm{t,AUV}}$ towards $\mathbf{p}_{\mathrm{d,AUV}}$ will begin. On the other hand, when the vessels tracks their targets with an accuracy lower than the one allowed by $\Delta_{\tilde{\mathbf{p}}_{\mathrm{t,USV}}}$ and $\Delta_{\tilde{\mathbf{p}}_{\mathrm{t,AUV}}}$, the rendezvous functions becomes $\rho_{\mathrm{USV}}(t) \approx 1$ and $\rho_{\mathrm{AUV}}(t) \approx 1$ which allows a safe and proper convergence of $\varpi_{\mathrm{t,AUV}}$. This is illustrated in Figure 5.5 with three different choices on Δ.

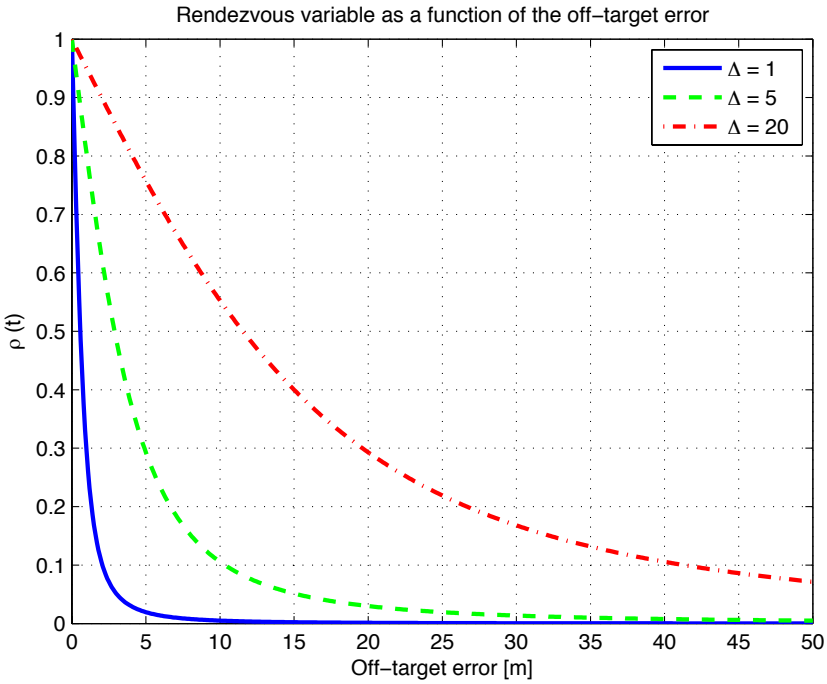

Figure 5.5: Profile of the rendezvous variable given the off-target error, with three different choices on Δ.

Proof of convergence

In this docking scenario it is desirable to have convergence of the target $\mathbf{p}_{\mathrm{t,AUV}}$, towards the docking point $\mathbf{p}_{\mathrm{d,AUV}}$, i.e.

$$\lim_{t\to\infty}(\mathbf{p}_{\mathrm{d,AUV}}(t)-\mathbf{p}_{\mathrm{t,AUV}}(t))=0. \tag{5.12}$$

Sometimes it is desirable with a medial offset on the docking point, such that $\varpi_{\mathrm{d}}\neq 0$. This then gives the general criteria to prove

$$\lim_{t\to\infty}\tilde{\varpi}_{\mathrm{t}}=0. \tag{5.13}$$

Here it is assumed perfect target tracking i.e. $\rho(t)\approx 1$, such that the target movement law in (5.6) can be simplified to

$$\dot{\varpi}_{\mathrm{t,AUV}}=\mathrm{U}_{\mathrm{t,a,max}}\frac{\tilde{\varpi}_{\mathrm{t}}}{\sqrt{\tilde{\varpi}_{\mathrm{t}}^2+\Delta_{\tilde{\varpi}_{\mathrm{t}}}^2}}. \tag{5.14}$$

To prove a general convergence, the following Lyapunov function candidate is chosen as

$$V(\tilde{\varpi}_{\mathrm{t}})=\frac{1}{2}\tilde{\varpi}_{\mathrm{t}}^2>0\quad\forall\ \tilde{\varpi}_{\mathrm{t}}\neq 0, \tag{5.15}$$

which clearly satisfies the conditions in Lyapunov's stability theorem. Then taking the time derivative such that

$$\dot{V}(\tilde{\varpi}_{\mathrm{t}})=\tilde{\varpi}_{\mathrm{t}}\dot{\tilde{\varpi}}_{\mathrm{t}}=\tilde{\varpi}_{\mathrm{t}}(\dot{\varpi}_{\mathrm{d}}-\dot{\varpi}_{\mathrm{t,AUV}}) \tag{5.16}$$

$$=\tilde{\varpi}_{\mathrm{t}}\left(-\mathrm{U}_{\mathrm{t,a,max}}\frac{\tilde{\varpi}_{\mathrm{t}}}{\sqrt{\tilde{\varpi}_{\mathrm{t}}^2+\Delta_{\tilde{\varpi}_{\mathrm{t}}}^2}}\right) \tag{5.17}$$

$$=-\mathrm{U}_{\mathrm{t,a,max}}\frac{\tilde{\varpi}_{\mathrm{t}}^2}{\sqrt{\tilde{\varpi}_{\mathrm{t}}^2+\Delta_{\tilde{\varpi}_{\mathrm{t}}}^2}}<0, \tag{5.18}$$

which clearly is negative definite and consequently providing a *uniformly globally asymptotically stable* (UGAS) approach towards the docking point.

During this proof, perfect target tracking was assumed which may not always be the case, but as long as $\rho(t)\neq 0$ the system will still be UGAS since

$$\dot{V}(\tilde{\varpi}_{\mathrm{t}})=-\mathrm{U}_{\mathrm{t,a,max}}\rho(t)\frac{\tilde{\varpi}_{\mathrm{t}}^2}{\sqrt{\tilde{\varpi}_{\mathrm{t}}^2+\Delta_{\tilde{\varpi}_{\mathrm{t}}}^2}}<0, \tag{5.19}$$

where $0<\rho(t)\leq 1$. In the case when $\rho(t)=0$, the objective will not be to have convergence of the target points, since this would cause an uncontrolled docking and which can result in damages to both the vehicles.

The docking method derived here can be summarised in three different stages, namely

Homing stage
USV begins to track the AUV's position with pure pursuit guidance, while the AUV stays passive in the water.

Docking stage: Inactive AUV
USV starts to track its new virtual target along a straight parameterized path, while the AUV still stays passive in the water.

Docking stage: Active AUV
USV tracks its target properly, and the AUV has the responsibility to complete the docking with the tracking of its virtual target.

5.2 USV to Mothership Docking

Another docking scenario of interest is the possibility to dock a USV against a manned mothership, without the interference from the mothership. This docking scenario is also divided into two stages, a homing stage and a docking stage. Here, both vessels are active during both stages, and the main docking task is carried out by the USV itself. The primary objectives for the mothership is to initialise docking such that the USV can start the docking procedure, and then traverse along a straight path without any sudden movements.

5.2.1 Homing Stage

In the beginning of a docking task the relative distance between the two vessels can be vast, compared to the precise accuracy in the final phase, and in this case there is a need to shorten this distance. How this is executed is called the homing stage and is carried out by the USV itself. To initiate the docking procedure the mothership signals the USV to confirm that the mothership is ready for docking, and therefore will not be making any sudden velocity changes. Once the USV receives this confirmation from the mothership it starts to converge towards the point $\mathbf{p}_{\text{f,USV}}$ by utilising a CB guidance scheme. The target point $\mathbf{p}_{\text{f,USV}}$ is illustrated in Figure 5.6 and given as

$$\mathbf{p}_{\text{f,USV}}(t) = \mathbf{p}_{\text{M}}(t) + \mathrm{l_c}\frac{\mathbf{p}_{\text{USV}}(t) - \mathbf{p}_{\text{M}}(t)}{||\mathbf{p}_{\text{USV}}(t) - \mathbf{p}_{\text{M}}(t)||}, \tag{5.20}$$

where $\mathrm{l_c}$ is the constant radius of the convergence circle, $\mathbf{p}_{\text{M}}$ is the position of the mothership, and $\mathbf{p}_{\text{USV}}$ is the position of the USV. When the USV has converged to the point $\mathbf{p}_{\text{f,USV}}$, the homing stage finishes and the docking stage takes over.

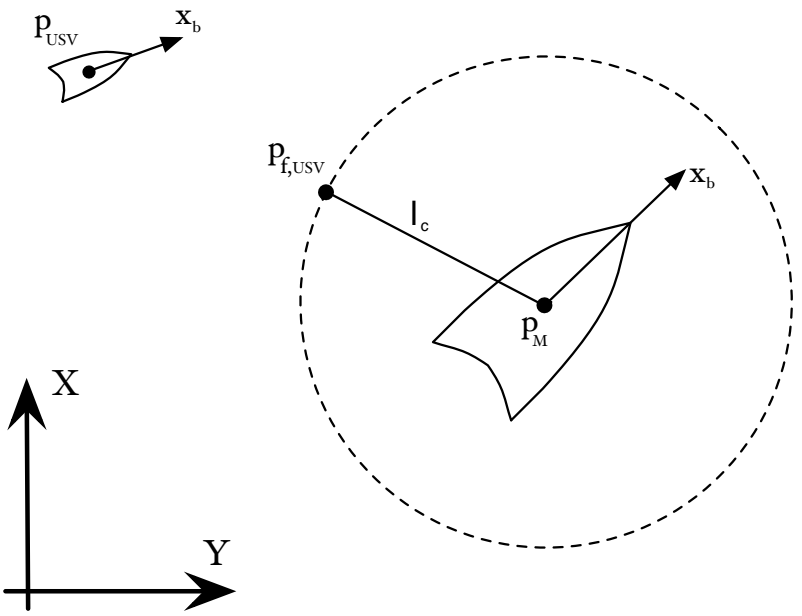

Figure 5.6: An illustration of the homing stage during the USV to mothership scenario.

5.2.2 Docking Stage

The docking stage begins once the USV has converged to the homing point $\mathbf{p}_{\mathrm{f,USV}}$, which is illustrated in Figure 5.6. During the docking stage relative distance between the two vehicles are short, and therefore more precise guidance laws are needed. The USV converges therefore first to a tracking circle where it needs to manoeuvre itself towards the docking point, which could be located on the other side of the mothership. To avoid collision with the mothership the USV starts to track the point $\mathbf{p}_{\mathrm{t,USV}}$ which is illustrated in Figure 5.7 and given by

$$\mathbf{p}_{\mathrm{t,USV}}(\varpi_{\mathrm{t}}, \gamma_{\mathrm{t}}) = \mathbf{p}_{\mathrm{M}}(t) + \varpi_{\mathrm{t}} \begin{bmatrix} \cos(\gamma_{\mathrm{t}} + \psi_{\mathrm{M}}) \\ \sin(\gamma_{\mathrm{t}} + \psi_{\mathrm{M}}) \end{bmatrix}, \tag{5.21}$$

where $\mathbf{p}_{\mathrm{M}}$ is the mothership's position, ϖ_{t} is a scalar parameter which defines the radius of the tracking circle with the initial condition $\varpi_{\mathrm{t}}(0) = l_{\mathrm{c}}$, and γ_{t} is the angle of the tracking point given according to the mothership's body-frame.

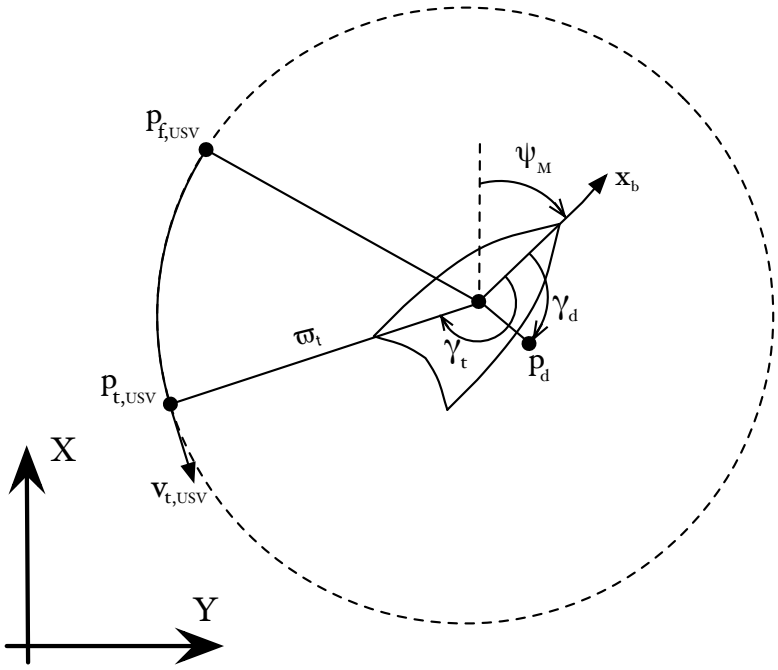

Figure 5.7: An illustration of the USV's target point $\mathbf{p}_{\mathrm{t,USV}}$ relative to the mothership.

The scalar values γ_{t} and ϖ_{t} in (5.21) generates the targets motion towards the docking point, and are updated through their separate target movement laws

$$\dot{\gamma}_{\mathrm{t}} = \mathrm{r}_{\mathrm{t,max}} \rho_{\mathrm{USV}}(t) \frac{\tilde{\gamma}_{\mathrm{t}}}{\sqrt{\tilde{\gamma}_{\mathrm{t}}^2 + \Delta_{\tilde{\gamma}_{\mathrm{t}}}^2}} \tag{5.22}$$

and

$$\dot{\tilde{\varpi}}_{\mathrm{t}} = \mathrm{U}_{\mathrm{t,max}} \rho_{\gamma_{\mathrm{t}}}(t) \rho_{\mathrm{USV}}(t) \frac{\tilde{\varpi}_{\mathrm{t}}}{\sqrt{\tilde{\varpi}_{\mathrm{t}}^2 + \Delta_{\tilde{\varpi}_{\mathrm{t}}}^2}}, \tag{5.23}$$

where $\mathrm{r}_{\mathrm{t,max}}$ and $\mathrm{U}_{\mathrm{t,max}}$ are the maximum angular and linear speed for the USV's virtual target $\mathbf{p}_{\mathrm{t,USV}}$, $\tilde{\gamma}_{\mathrm{t}} \triangleq \gamma_{\mathrm{d}} - \gamma_{\mathrm{t}} \in [-\pi\,, \pi]$ is the angular difference between the virtual target $\mathbf{p}_{\mathrm{t,USV}}$ and the docking point $\mathbf{p}_{\mathrm{d}}$, $\rho_{\gamma_{\mathrm{t}}(t)}$ and $\rho_{\mathrm{USV}}(t)$ are the rendezvous variables, and $\tilde{\varpi}_{\mathrm{t}} \triangleq l_{\mathrm{d}} - \varpi_{\mathrm{t}}$ is the linear difference between the target point $\mathbf{p}_{\mathrm{t,USV}}$ and the docking point $\mathbf{p}_{\mathrm{d}}$, where l_{d} is the length between the mothership's position and the docking point.

The rendezvous variables $\rho_{\gamma_t(t)}$ and $\rho_{\text{USV}}(t)$ are introduced to prevent an uncontrolled behaviour of the virtual target, and are given as

$$\rho_{\gamma_t}(t) = \left(1 - \frac{|\tilde{\gamma}_t(t)|}{\sqrt{\tilde{\gamma}_t^2(t) + \Delta_{\rho,\tilde{\gamma}}^2}}\right) \tag{5.24}$$

and

$$\rho_{\text{USV}}(t) = \left(1 - \frac{|\tilde{\mathbf{p}}_{t,\text{USV}}(t)|}{\sqrt{\tilde{\mathbf{p}}_{t,\text{USV}}^T(t)\tilde{\mathbf{p}}_{t,\text{USV}}(t) + \Delta_{\rho,\tilde{\mathbf{p}}}^2}}\right). \tag{5.25}$$

Here,

$$\tilde{\mathbf{p}}_{t,\text{USV}}(t) \triangleq \mathbf{p}_{t,\text{USV}}(t) - \mathbf{p}_{\text{USV}}(t) \tag{5.26}$$

is the line of sight vector between the USV and its virtual target $\mathbf{p}_{t,\text{USV}}$. When the distance between the USV and its virtual target is greater than $\Delta_{\rho,\tilde{\mathbf{p}}}$, the rendezvous function involving the USV becomes $\rho_{\text{USV}}(t) \approx 0$, which forbids an update of both the target movement laws. An update of γ_t will only happen when the USV track its target with an accuracy given according to $\Delta_{\rho,\tilde{\mathbf{p}}}$, see Figure 5.5. Since $\dot{\varpi}_t$ also depends on $\rho_{\gamma_t}(t)$, the virtual target is constrained to the tracking circle until $\tilde{\gamma}_t \approx 0$, and therefore the USV will avoid collisions with the mothership. Once $\tilde{\gamma}_t \approx 0$ such that $\rho_{\gamma_t}(t) \approx 1$, the USV starts to converge towards the mothership and the docking point to finalise the docking.

In the final docking stage when $\tilde{\gamma}_t \approx 0$, the scalar value $\tilde{\varpi}_t$ starts to converge towards zero. During this stage, the relationship between the mothership's forward speed and the convergence speed of the target point $\mathbf{p}_{t,\text{USV}}$ has to be well planned such that the USV does not approach the mothership with a skew orientation. The reason for this is that the USV is underactuated in this situation, which mean that it can not control it's velocity vector independently from an arbitrary orientation. The USV must therefore compensate the sideway motion throughout its surge speed and heading. This manoeuvre forces a slant heading from the USV compared to the mothership, and is correlated with the mothership's forward speed and the convergence speed of the target point, which is illustrated in Figure 5.8. The USV's approach angle in this phase can easily be described by

$$\beta = \text{atan}\left(\frac{\text{U}_\text{a}}{\text{U}_\text{M}}\right), \tag{5.27}$$

where U_a is the relative approach speed towards the docking point, and U_M is the speed of the mothership. The approach speed will vary from a maximum in the beginning, towards a minimum in the end and consequently the angle will therefore also vary because the speed of the mothership stays constant. It is therefore desirable to have a small approach speed towards the end and a higher approach speed in the beginning. This behaviour can be tuned through the parameters $U_{t,max}$ and $\Delta_{\tilde{\varpi}_t}$ in Equation (5.23).

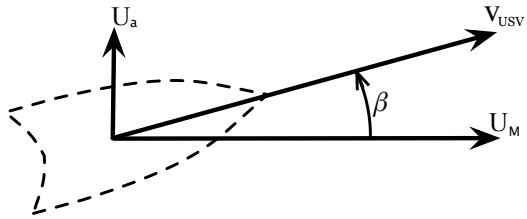

Figure 5.8: An illustration of the USV's approach angle towards the mothership.

Proof of convergence

In the USV to mothership docking scenario the objective is that the USV's position $\mathbf{p}_{t,USV}(t)$ has to converge towards the docking station's position $\mathbf{p}_d(t)$, i.e.

$$\lim_{t\to\infty} (\mathbf{p}_d(t) - \mathbf{p}_{t,USV}(t)) = 0, \tag{5.28}$$

where

$$\mathbf{p}_d(t) = \mathbf{p}_M(t) + l_d \begin{bmatrix} \cos(\gamma_d + \psi_M) \\ \sin(\gamma_d + \psi_M) \end{bmatrix}. \tag{5.29}$$

To achive (5.28), both the scalar values has to converge towards zero i.e.

$$\lim_{t\to\infty} \tilde{\varpi}_t = 0 \quad \text{and} \quad \lim_{t\to\infty} \tilde{\gamma}_t = 0, \tag{5.30}$$

which then becomes the criterias to prove.

Assuming perfect target tracking such that $\rho_{\gamma_t}(t) = \rho_{USV}(t) = 1$ and a rigidly attached docking point such that $l_d = constant$ and $\gamma_d = constant$, gives the following simplified target movement laws from (5.22) and (5.23)

$$\dot{\gamma}_t = r_{t,max} \frac{\tilde{\gamma}_t}{\sqrt{\tilde{\gamma}_t^2 + \Delta_{\tilde{\gamma}_t}^2}} \tag{5.31}$$

and

$$\dot{\varpi}_{\mathrm{t}} = \mathrm{U}_{\mathrm{t,max}} \frac{\tilde{\varpi}_{\mathrm{t}}}{\sqrt{\tilde{\varpi}_{\mathrm{t}}^2 + \Delta_{\tilde{\varpi}_{\mathrm{t}}}^2}}. \tag{5.32}$$

To prove $\lim_{x\to\infty} x = 0$ with the given state space vector $x = [\tilde{\gamma}_{\mathrm{t}}\,,\, \tilde{\varpi}_{\mathrm{t}}]^T$, the Lyapunov candidate function is chosen as

$$V(x) = \frac{1}{2} x x^T > 0 \quad \forall\, x \neq 0, \tag{5.33}$$

which is according to Lyapunov's stability theorem. Then taking the time derivative of $V(x)$ which gives

$$\dot{V}(x) = x\dot{x}^T = \tilde{\gamma}_{\mathrm{t}}\dot{\tilde{\gamma}}_{\mathrm{t}} + \tilde{\varpi}_{\mathrm{t}}\dot{\tilde{\varpi}}_{\mathrm{t}} \tag{5.34}$$

$$= \tilde{\gamma}_{\mathrm{t}}(\dot{\gamma}_{\mathrm{d}} - \dot{\gamma}_{\mathrm{t}}) + \tilde{\varpi}_{\mathrm{t}}(\dot{l}_{\mathrm{d}} - \dot{\varpi}_{\mathrm{t}}) \tag{5.35}$$

$$= -\mathrm{r}_{\mathrm{t,max}} \frac{\tilde{\gamma}_{\mathrm{t}}^2}{\sqrt{\tilde{\gamma}_{\mathrm{t}}^2 + \Delta_{\tilde{\gamma}_{\mathrm{t}}}^2}} - \mathrm{U}_{\mathrm{t,max}} \frac{\tilde{\varpi}_{\mathrm{t}}^2}{\sqrt{\tilde{\varpi}_{\mathrm{t}}^2 + \Delta_{\tilde{\varpi}_{\mathrm{t}}}^2}} < 0. \tag{5.36}$$

This is negative definite and therefore provides a UGAS docking approach.

Also in this proof perfect target tracking was assumed, but as long as $\rho_{\gamma_{\mathrm{t}}}(t) = \rho_{\mathrm{USV}}(t) \neq 0$ it can also be noted here that

$$\dot{V}(x) = -\mathrm{r}_{\mathrm{t,max}}\rho_{\mathrm{USV}}(t) \frac{\tilde{\gamma}_{\mathrm{t}}^2}{\sqrt{\tilde{\gamma}_{\mathrm{t}}^2 + \Delta_{\tilde{\gamma}_{\mathrm{t}}}^2}} - \mathrm{U}_{\mathrm{t,max}}\rho_{\gamma_{\mathrm{t}}}(t)\rho_{\mathrm{USV}}(t) \frac{\tilde{\varpi}_{\mathrm{t}}^2}{\sqrt{\tilde{\varpi}_{\mathrm{t}}^2 + \Delta_{\tilde{\varpi}_{\mathrm{t}}}^2}} < 0, \tag{5.37}$$

where $0 < \rho_{\gamma_{\mathrm{t}}}(t) \leq 1$ and $0 < \rho_{\mathrm{USV}}(t) \leq 1$ will provide UGAS. It must also be noted here that when $\rho_{\gamma_{\mathrm{t}}}(t) = 0$ or $\rho_{\mathrm{USV}}(t) = 0$, the objective will not be to have convergence of the target point, since this will result in an improper docking where collisions could occur.

The USV to mothership scenario derived here can be summarised into the three subsystems

Homing stage
The USV tracks the homing point $\mathbf{p}_{\mathrm{f,USV}}$ located on tracking circle where the line of sight vector between the USV and the mothership crosses.

Docking stage: Tracking circle
The USV has converged to the tracking circle and begins to manoeuvre along the circle to avoid collisions with the mothership.

Docking stage: Final docking
The USV has straight line towards the docking point and begins to converge towards the mothership to complete docking.

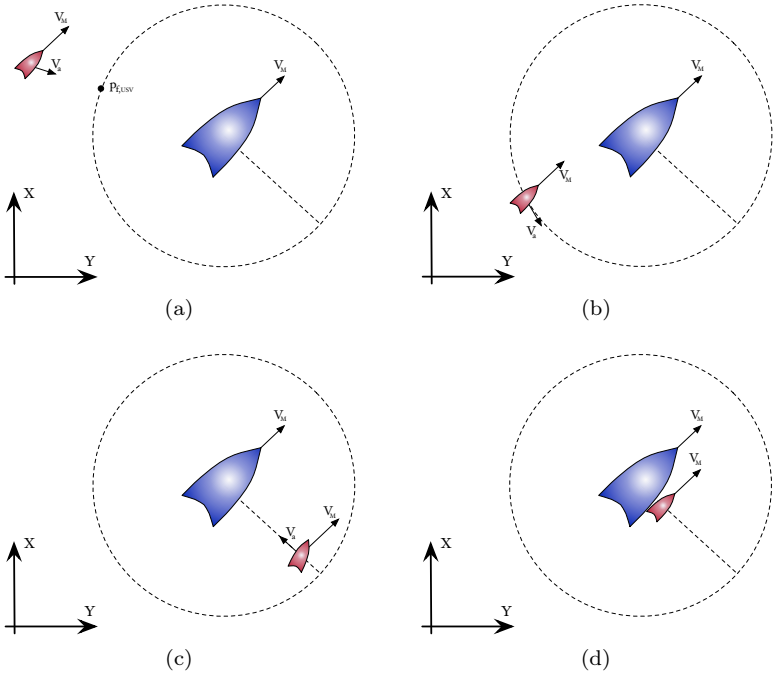

Figure 5.9: USV to mothership docking sequence. (a) shows the homing stage, (b) shows the manoeuvre along the tracking circle, (c) shows the sideway convergence towards the docking station, and (d) shows the USV docking together with the mothership.

Chapter 6

Velocity Control System

In Chapter 5 the target-tracking for two docking scenarios was derived. These two target-tracking scenarios employ a CB guidance scheme, where the velocity command is given in (4.2). The two docking scenarios are designed for underactuated vessels, and therefore the velocity command from the CB guidance cannot be used directly. This chapter details the velocity control system that enables an underactuated vessel to achieve the given velocity command required to attain the target tracking control objectives derived above. When underactuated vessels are treated the sway speed $v(t)$ cannot be directly controlled, and consequently the velocity command has to be divided between surge speed and yaw rate controllers. The material from this chapter comes mainly from (Breivik et al., 2008).

6.1 Surge Speed Controller

When the velocity command is divided between surge controller and yaw rate controller, the surge controller becomes responsible for controlling the size of the velocity vector $\mathbf{v}(t)$, while the yaw rate controller is responsible for controlling the direction of the velocity, see Figure 6.1. The speed error is denoted as

$$\tilde{\mathrm{U}}(t) \triangleq \mathrm{U_d}(t) - \mathrm{U}(t), \tag{6.1}$$

where $\mathrm{U_d}(t) \triangleq |\mathbf{v}_\mathrm{d}(t)|$ with $\mathbf{v}_\mathrm{d}(t)$ as the assigned velocity $\mathbf{v}(t)$ from the CB guidance in (4.2). The objective of the speed control then becomes

$$\lim_{t\to\infty} \tilde{\mathrm{U}}(t) = 0, \tag{6.2}$$

which needs to be rewrote into terms of corresponding control objective for the surge speed. Since $\mathrm{U}(t) = |\mathbf{v}(t)| = \sqrt{u(t)^2 + v(t)^2}$ and (6.2) states that the goal

is to have $\mathrm{U}(t) \to \mathrm{U_d}(t)$, which becomes $\sqrt{u(t)^2 + v(t)^2} \to \mathrm{U_d}(t)$ or equivalently that $u(t) \to \sqrt{\mathrm{U_d}(t)^2 - v(t)^2}$. The desired surge speed is then defined as

$$u_{\mathrm{d}}(t) \triangleq \sqrt{\mathrm{U_d}(t)^2 - v(t)^2}, \tag{6.3}$$

which is valid when assuming $\mathrm{U_d}(t) \leq |v(t)|$ at all times, which is highly realistic since in practice $|v(t)|$ is just a small fraction of $\mathrm{U}(t)$ for straight-line motion at high speeds.

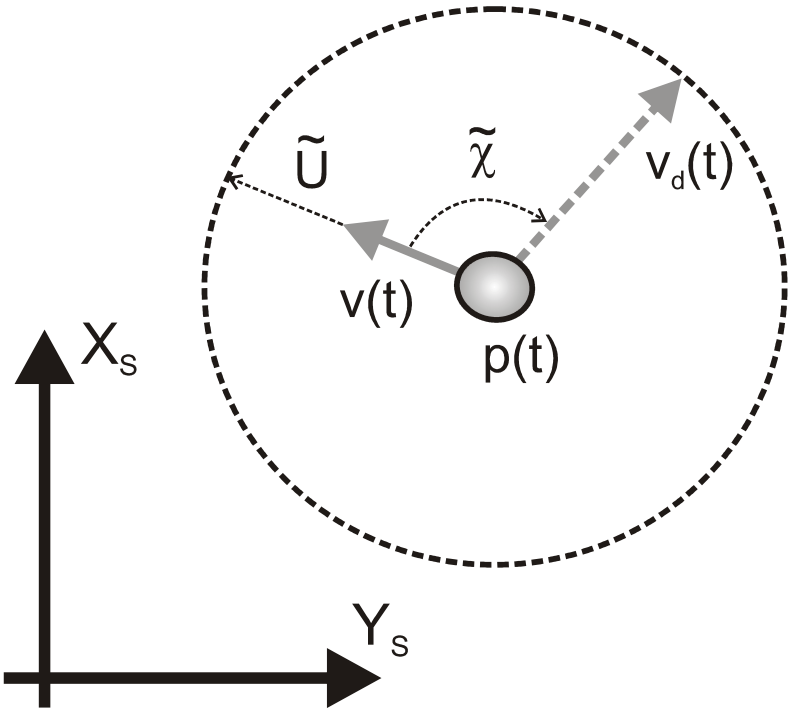

Figure 6.1: The decomposition of the velocity error $\tilde{\mathbf{v}}(t)$ into a speed error $\tilde{\mathrm{U}}$ and a course error $\tilde{\chi}$. Courtesy of Breivik et al. (2008)

6.2 Yaw Rate Controller

The responsibility of the yaw rate controller is to make the direction of the vessel velocity match the direction of the velocity assignment given by the guidance system. The velocity direction is denoted as the course, where the course error is given as

$$\tilde{\chi}(t) \triangleq \chi_{\mathrm{d}}(t) - \chi(t), \tag{6.4}$$

where $\chi_{\mathrm{d}}(t) \triangleq \operatorname{atan2}(\dot{y}_{\mathrm{d}}(t), \dot{x}_{\mathrm{d}}(t))$ represents the desired course angle of $\mathbf{v}_{\mathrm{d}}$, and $\chi(t) \triangleq \operatorname{atan2}(\dot{y}(t), \dot{x}(t))$ represents the actual course angle of the vessel. The objective of the course control becomes

$$\lim_{t\to\infty} \tilde{\chi}(t) = 0, \tag{6.5}$$

which together with the control objective for the surge speed controller enables a fulfilment of a target-tracking scenario.

The course error $\tilde{\chi}(t)$ can be calculated according to (6.4), but this can cause wraparound problems. To avoid these wraparound problems, $\tilde{\chi}(t)$ can be calculated directly by

$$\tilde{\chi}(t) = \operatorname{atan2}(\sin(\tilde{\chi}(t)), \cos(\tilde{\chi}(t))), \tag{6.6}$$

where $\sin(\tilde{\chi}(t))$ and $\cos(\tilde{\chi}(t))$ are computed by employing the cross- and inner-product information about the velocities $\mathbf{v}_{\mathrm{d}}(t)$ and $\mathbf{v}(t)$, which are given according to

$$\mathbf{v}(t) \times \mathbf{v}_{\mathrm{d}}(t) = |\mathbf{v}(t)||\mathbf{v}_{\mathrm{d}}(t)| \sin(\tilde{\chi}(t)) = \mathrm{U}(t)\mathrm{U}_{\mathrm{d}}(t) \sin(\tilde{\chi}(t)) \tag{6.7}$$

and

$$\mathbf{v}(t) \cdot \mathbf{v}_{\mathrm{d}}(t) = |\mathbf{v}(t)||\mathbf{v}_{\mathrm{d}}(t)| \cos(\tilde{\chi}(t)) = \mathrm{U}(t)\mathrm{U}_{\mathrm{d}}(t) \cos(\tilde{\chi}(t)). \tag{6.8}$$

The employed desired yaw rate is then given by

$$r_{\mathrm{d}}(t) = r_{\mathrm{a,max}} \tanh\left(\frac{k_{\mathrm{p},\tilde{\chi}} \tilde{\chi}(t)}{r_{\mathrm{a,max}}}\right), \tag{6.9}$$

where $r_{\mathrm{a,max}}$ represents the maximum available yaw rate from the given vessel and $k_{\mathrm{p},\tilde{\chi}} > 0$ shapes the desired yaw rate and is illustrated in Figure 6.2. This figure shows how different choices on the gain $k_{\mathrm{p},\tilde{\chi}}$ shapes the desired yaw rate, where a large value results in a steep approach, and smaller values gives a much smoother approach.

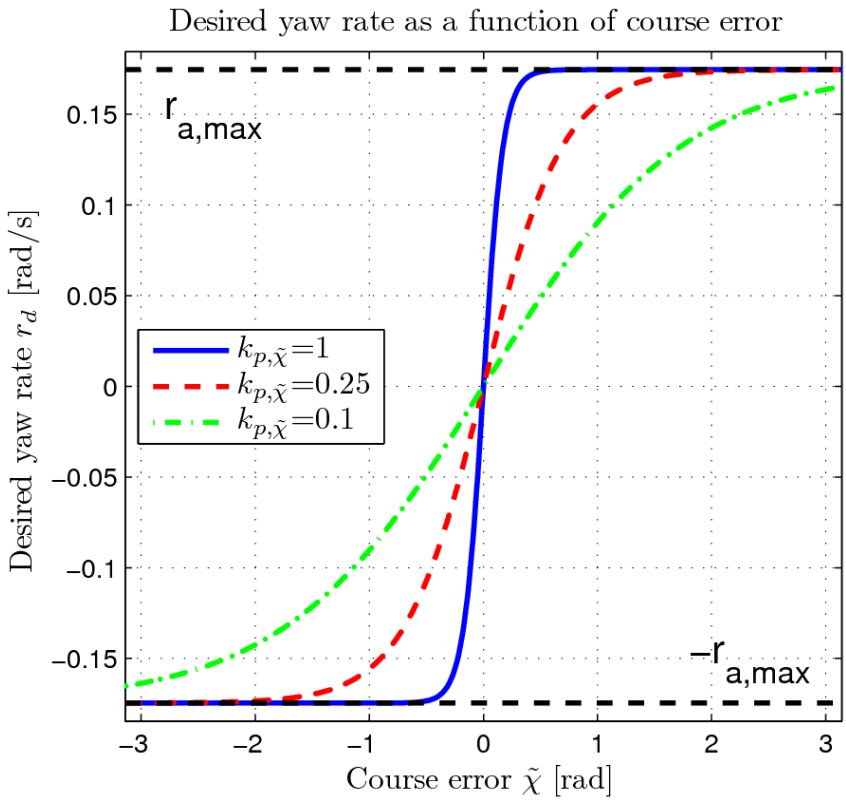

Figure 6.2: Profile of the desired yaw rate given as a function of the course error, with three different choices on $k_{\mathrm{p},\tilde{\chi}}$. Courtesy of Breivik et al. (2008)

Chapter 7

Simulation Results

In Chapter 5 two docking scenarios, AUV to USV and USV to mothership was presented. These scenarios include the docking of unmanned marine vessel without human interference. The main subject was the guidance laws which will allow a safe and proper docking. Throughout this chapter simulations are presented to analyse each docking scenarios properly.

7.1 AUV to USV Docking

The AUV to USV docking scenario was presented in Section 5.1, and here simulations are carried out to study the behaviour between the two vessels. The simulations are based on the assumptions of an open sea without nearby obstacles, no external forces or disturbances. The models used here are USV models of two underactuated vessels, with controllability over surge speed and yaw rate. Further it is assumed that a successful docking is achieved once the AUV reaches a predefined docking point with the correct heading. At last the wind direction which the docking path is aligned against is given as a predefined angle which specifies the docking path, since theres no external disturbances.

7.1.1 Implementation

The AUV to USV docking scenario is implemented in Matlab/Simulink, and the solver used is *ode15s* with a maximum step length of $0.1s$ to assure an accurate solution. The vessel models used are 3DOF velocity-controlled models of the Viknes USV and the Mariner USV, where details on the velocity control system can be found in (Breivik et al., 2008). Due to the lack of AUVs in the Trondheim district, the Mariner USV will be employed as an AUV throughout these

simulations. These models have the following upper bounds on surge speed and rotation rate

$$\text{Viknes USV:} \quad \mathrm{U}_{\max} = 8.9\, m/s \quad r_{\max} = 0.41\, m/s$$

$$\text{Mariner USV:} \quad \mathrm{U}_{\max} = 5.5\, m/s \quad r_{\max} = 0.35\, m/s.$$

To control these models the following parameters are chosen for the control model:

Viknes USV:		
CB Guidance System:	$\mathrm{U}_{\mathrm{a,max}} = 3\, m/s$	$\Delta_{\tilde{\mathbf{p}},\mathrm{USV}} = 120$
Velocity Control Model:	$r_{\mathrm{a,max}} = 0.3075\, m/s$	$k_{p,\tilde{\chi}} = 0.1.$

Mariner USV:		
CB Guidance System:	$\mathrm{U}_{\mathrm{a,max}} = 2\, m/s$	$\Delta_{\tilde{\mathbf{p}},\mathrm{USV}} = 85$
Velocity Control Model:	$r_{\mathrm{a,max}} = 0.2625\, m/s$	$k_{p,\tilde{\chi}} = 0.15.$

During the following simulations the homing circle which marks the boundary between homing and docking stage is chosen to 100 metres, where the circle that activates the AUV is chosen to 25 metres. The parameters that locates the docking station are selected as $l_{\mathrm{d}} = 10$ metres and $\alpha_{\mathrm{d}} = \pi$, which places the docking station 10 metres behind the aft of the USV when the off-set parameter ϖ_{d} equals zero.

Furthermore the parameters that specifies the target behaviour are summed up as:

$$\mathrm{U}_{\mathrm{t,USV}} = 3\, m/s, \quad \varpi_{\mathrm{USV}}(0) = 0, \quad \varpi_{\mathrm{AUV}}(0) = -30, \tag{7.1}$$

$$\mathrm{U}_{\mathrm{t,a,max}} = 6\, m/s, \quad \Delta_{\tilde{\varpi}_{\mathrm{t}}} = 100, \quad \Delta_{\tilde{\mathbf{p}}_{\mathrm{t,AUV}}} = 1, \quad \text{and} \quad \Delta_{\tilde{\mathbf{p}}_{\mathrm{t,USV}}} = 3. \tag{7.2}$$

At last the wind direction is chosen as $\alpha_{\mathrm{wind}} = 225°$ which will give the docking path an orientation of 45°.

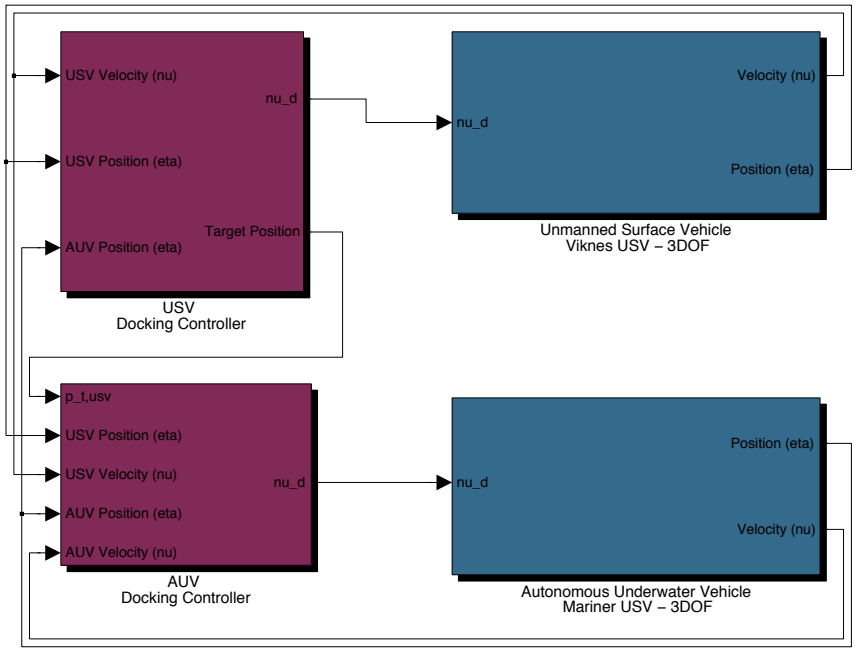

Figure 7.1: The top level Simulink diagram for the AUV to USV docking scenario.

7.1.2 Results

The total simulation lasts for 400 s, where in Figure 7.2 a NED-frame plot of the homing stage and early docking stage is shown. In the homing stage one can observe how the USV chooses $\mathbf{p}_{\mathrm{f},3}$ as the fixed point on the parametrizated path once it enters the homing circle, which is correct from the definitions in Table 5.1 and Figure 5.1. The final docking stage is show in Figure 7.3, and during this stage it can be observed that the AUV peruses the USV from behind and therefore will approach the docking station with a desirable orientation.

In Figure 7.4 the off-target behaviour of the USV and AUV towards their respective targets are given, and in this figure it shows that both vessels converges nicely to their respective target points. Here the AUV is inactive before 98 s, which can be interpreted as the time when the USV has an off-target distance greater than 25 metres. Also the increase in the off-target distance during the beginning of each plot is because the vehicles starts with zero speed, and therefore needs some time to reach their desired speeds. This can be shown clearly in Figure 7.5, where the surge speed and yaw rate are given for both vessels.

The off-target behaviour of the AUV towards the docking point is shown in Figure 7.6. In this figure the part with the inactive AUV is left out, because this does not give any valuable information. From this figure it can be observed that the AUV converges nicely to the docking point without any overshoot. Together with Figure 7.5 it can be seen how the vessel slows down in the final metres to allow a smooth approach such that damages will not occur on neither of the vessels.

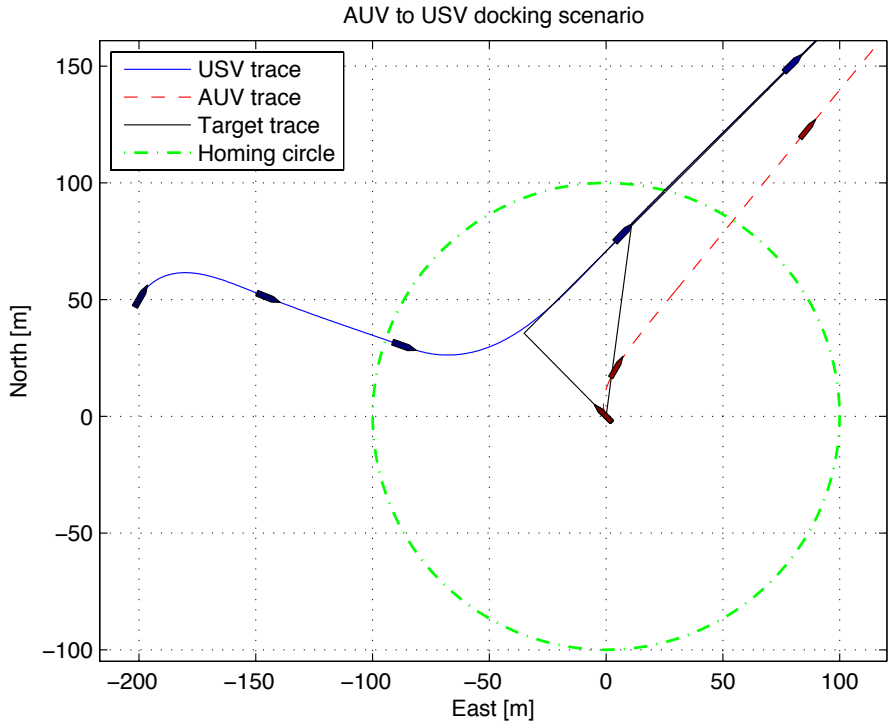

Figure 7.2: The homing stage for AUV to USV docking scenario, given in NED-frame.

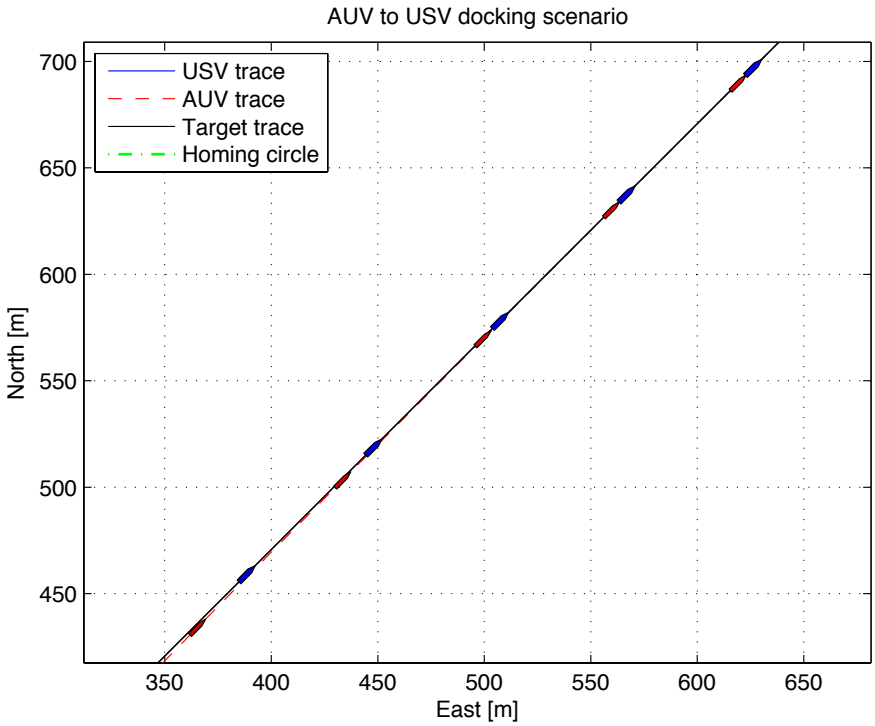

Figure 7.3: The final phase in the docking stage during the AUV to USV docking scenario, given in NED-frame.

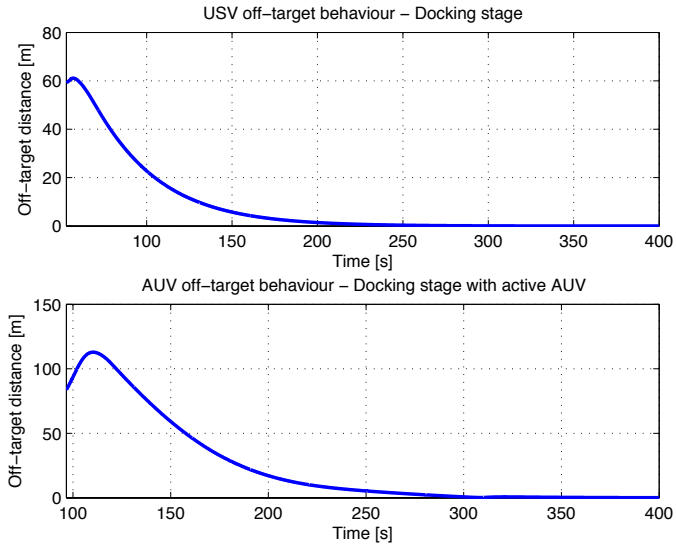

Figure 7.4: AUV and USV off-target behaviour towards their respective targets in the docking stage.

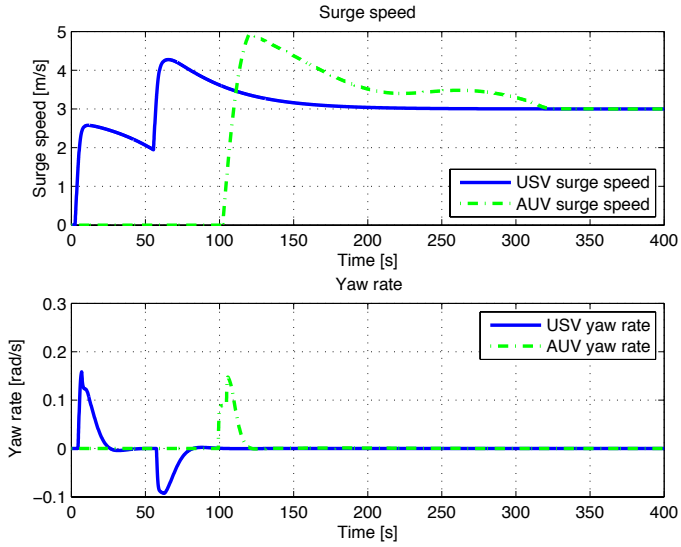

Figure 7.5: Surge speed and yaw rate.

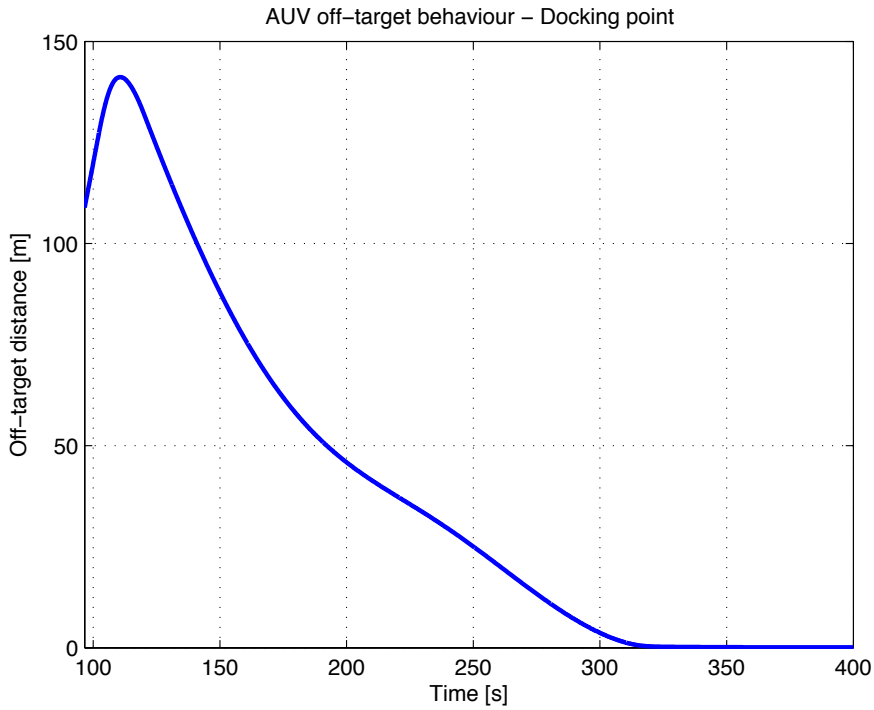

Figure 7.6: AUV off-target behaviour towards the docking point.

7.2 USV to Mothership Docking

In Section 5.2 the scenario for docking a USV against a mothership was presented, and in this section simulations are carried out to study the behaviour between the two vessels. During the simulations it is assumed an open sea without any nearby obstacles and no external forces or disturbances. It is also assumed that once the USV reaches the predefined docking point with a correct heading, successful docking is achieved. Further, the USV model used is an underactuated 3DOF velocity-controlled model of the Viknes USV, with controllability over surge speed and yaw rate. Details on the velocity control system can be found in (Breivik et al., 2008)

7.2.1 Implementation

This docking scenario is implemented and simulated in Matlab/Simulink, see Figure 7.7 for a top level Simulink diagram. The solver used is *ode*15*s* with a maximum step size of 0.1*s*, such that an accurate solution is obtained. The mothership traverses along a straight path and is given as a kinematic model, where the initial position is chosen relative to the USV, and are given as

$$\mathbf{p}_{\mathrm{M}}(0) = \mathbf{p}_{\mathrm{USV}}(0) + l_{\mathrm{r}}\mathbf{R}(\psi_{\mathrm{USV}}) \begin{bmatrix} \cos(\psi_{\mathrm{r}}) \\ \sin(\psi_{\mathrm{r}}) \end{bmatrix}, \tag{7.3}$$

where $\mathbf{p}_{\mathrm{USV}}$ is the USV's position, $\mathbf{R}(\psi_{\mathrm{USV}})$ is the 2-dimensional rotation matrix in yaw, l_{r} and ψ_{r} is the length and angle relative to the USV's body-frame. Since this is a pure kinematic model the position $\mathbf{p}_{\mathrm{M}}(t)$ is obtained through an integration of the velocity $\mathbf{v}_{\mathrm{M}} \triangleq [\dot{y}_{\mathrm{M}}, \dot{x}_{\mathrm{M}}]^T$, which is stated in the NED-frame and given by

$$\mathbf{v}_{\mathrm{M}}(t) = \mathrm{U}_{\mathrm{M}} \begin{bmatrix} \cos(\alpha) \\ \sin(\alpha) \end{bmatrix}, \tag{7.4}$$

where U_{M} is the speed with which the mothership traverses the path, and α is the angle of the mothership's path given relative to the NED-frame. Additionally, the heading angle is given as

$$\psi_{\mathrm{M}} = \mathrm{atan2}(\dot{y}_{\mathrm{M}}, \dot{x}_{\mathrm{M}}). \tag{7.5}$$

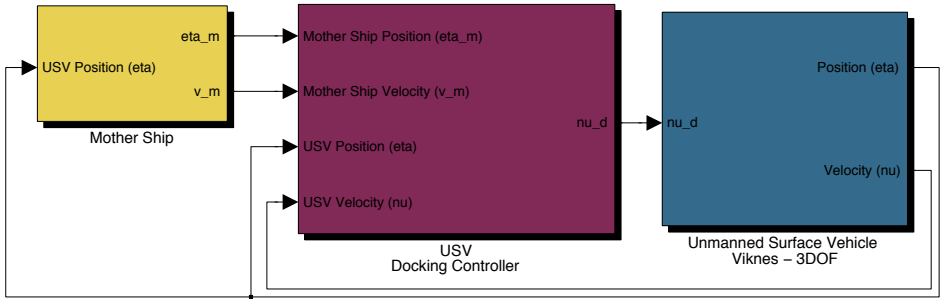

Figure 7.7: The top level Simulink diagram for the USV to mothership docking scenario.

During this simulation the following parameters are chosen for the mothership

$$l_{\mathrm{r}} = 100\,m, \quad \psi_{\mathrm{r}} = 90^{\circ}, \quad \mathrm{U_M} = 3\,m/s, \quad \text{and} \quad \alpha = 40^{\circ}. \tag{7.6}$$

The parameters related to the orientation of the docking station is chosen as

$$\gamma_{\mathrm{d}} = 90^{\circ} \quad \text{and} \quad l_{\mathrm{d}} = 5.29\,m, \tag{7.7}$$

which places the docking station 5.29 metres from the steering point on the starboard side of the mothership. Here it is assumed that the mothership has a width of 8 metres and the Viknes USV has the width of 2.57 metres. The choice of α_{d} and l_{d} will therefore align the two vehicles side by side.

The USV model used during the simulation is a model of the Viknes USV and the parameters related to this model are given by

$$\mathrm{U_{max}} = 8.9\,m/s \quad \text{and} \quad \mathrm{r_{max}} = 0.41\,rad/s, \tag{7.8}$$

with the following parameters for the control model:

CB Guidance System:	$\mathrm{U_{a,max}} = 3\,m/s$	$\Delta_{\tilde{\mathbf{p}},\mathrm{USV}} = 120$
Velocity Control Model:	$r_{\mathrm{a,max}} = 0.3075\,m/s$	$k_{p,\tilde{\chi}} = 0.2.$

The parameters for the virtual target which are explained in Section 5.2 are chosen as

$$\Delta_{\tilde{\gamma}_{\mathrm{t}}} = 1, \quad \Delta_{\rho,\tilde{\gamma}} = 2, \quad \mathrm{r_{t,max}} = 0.1\,rad/s, \tag{7.9}$$

$$\Delta_{\tilde{\varpi}_{\mathrm{t}}} = 10, \quad \Delta_{\rho,\tilde{\mathbf{p}}} = 2, \quad \text{and} \quad \mathrm{U_{t,max}} = 0.3\,m/s. \tag{7.10}$$

7.2.2 Results

The total simulation time lasts for $600\,s$ and in Figure 7.8, a 2-dimensional work space plot in NED coordinates is shown, where positions are relative to the mothership. In this plot the USV converges nicely to the homing circle, and from there manoeuvres towards the docking point where firstly $\tilde{\gamma}_{\mathrm{t}} \to 0$, and then $\tilde{\varpi}_{\mathrm{t}}$ starts to converge towards zero ensuring a safe and proper docking. One can also observe that the USV docks with a heading that equals the one of the mothership. The strange behaviour from the USV in the beginning comes from the fact that this is a plot relative to the mothership and that the USV starts with zero speed and so it needs some time to accelerate up to the desired speed which is not the case for the kinematic mothership.

By analysing the off-target behaviour in Figure 7.9 one clearly observes that the USV converges to both the virtual target and docking station in satisfying manners. The most important element in this plot, is that the USV does not approach the docking point with an overshoot, meaning that the USV would crash into the mothership. From the bottom plot in Figure 7.9 it can be noted that the USV does not have an overshoot in the approach towards the docking point.

The reason for the increasing off-target distance during the start-up phase in Figure 7.9 comes from the fact that the USV starts with zero speed. This comes clearly out from the surge speed plot in Figure 7.10. From the surge speed and off-target plot it can be seen that the USV approaches the mothership nice and slowly in the end.

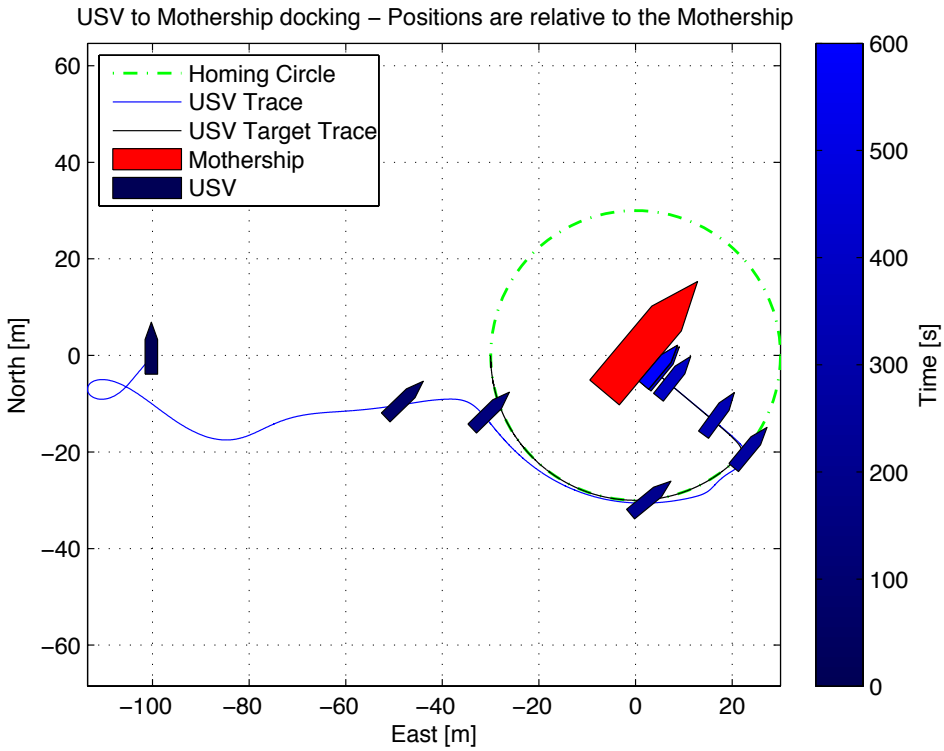

Figure 7.8: The USV closing upon the mothership and manoeuvres into docking position, with coordinates given relative to the mothership, and a colour bar to indicate simulation time.

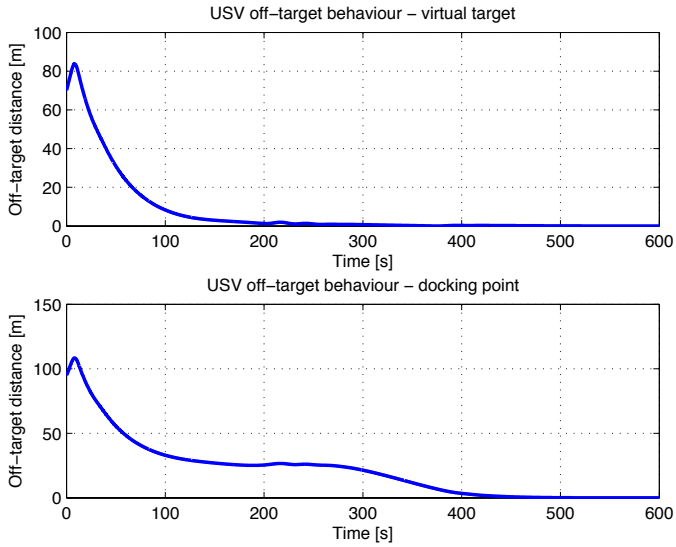

Figure 7.9: Off-target behaviour for the USV's position $\mathbf{p}_{\mathrm{USV}}$, towards the virtual target $\mathbf{p}_{\mathrm{t,USV}}$ and the docking station $\mathbf{p}_{\mathrm{dock}}$.

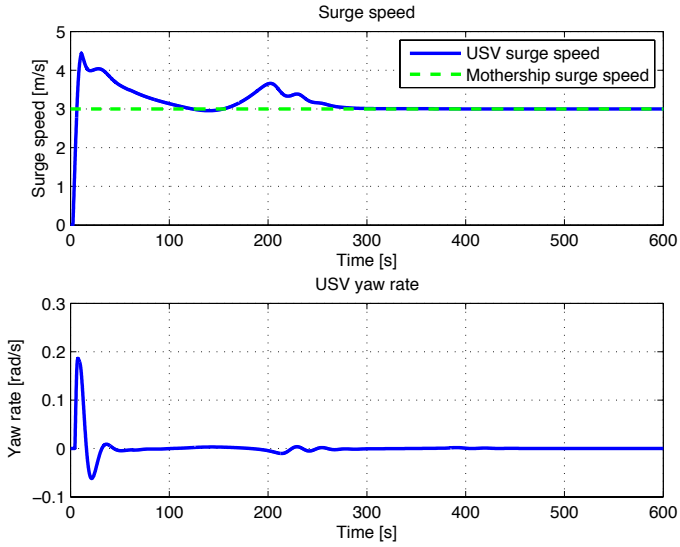

Figure 7.10: Surge speed and yaw rate.

Higher speed for the mothership

To see how the approach changes with the mothership's speed, another simulation is carried out. Here the mothership's speed is changed to $\mathrm{U_M} = 5\,m/s$ to show how this speed influences the USV's approach towards the mothership. Once the mothership travels with a higher speed, the target movement law in (5.23) can be tuned different such that the USV would approach the mothership faster without increase steering towards the mothership. The new parameters in (5.23) are now chosen as

$$\Delta_{\tilde{\varpi}_{\mathrm{t,d}}} = 17, \quad \text{and} \quad \mathrm{U_{t,max}} = 0.5\,m/s. \tag{7.11}$$

The simulation time is now shortened down to $500\,s$ and the 2-dimensional work space plot in NED coordinates is shown in Figure 7.11, where it can be seen that the USV approaches the mothership in the same satisfying manners as the previous case with $\mathrm{U_M} = 3\,m/s$. It also has to be noted that the "strange" behaviour from the USV in the beginning comes from the fact that the USV starts with zero speed, and this is a plot relative to the mothership.

From Figure 7.12 the USV's off-target behaviour towards the virtual target and docking point is shown. It can be seen together with the surge speed plot in Figure 7.13 that the USV also here approaches the docking point nicely without any overshoot.

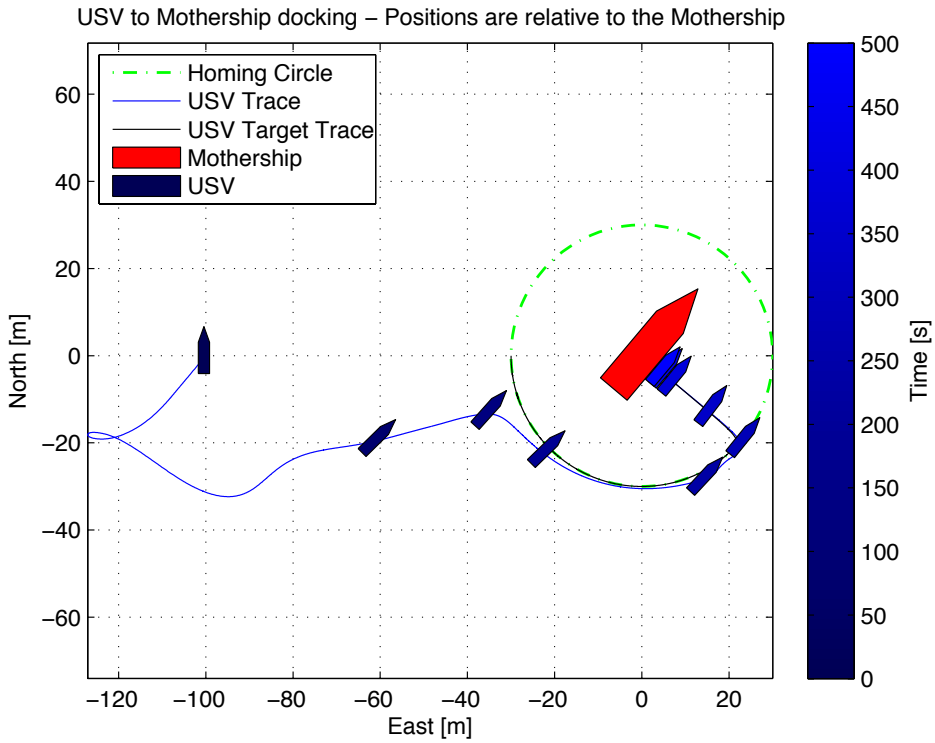

Figure 7.11: The USV closing upon the mothership and manoeuvres into docking position, with coordinates given relative to the mothership. The mothership speed is $5\,m/s$ and the colour bar indicate simulation time.

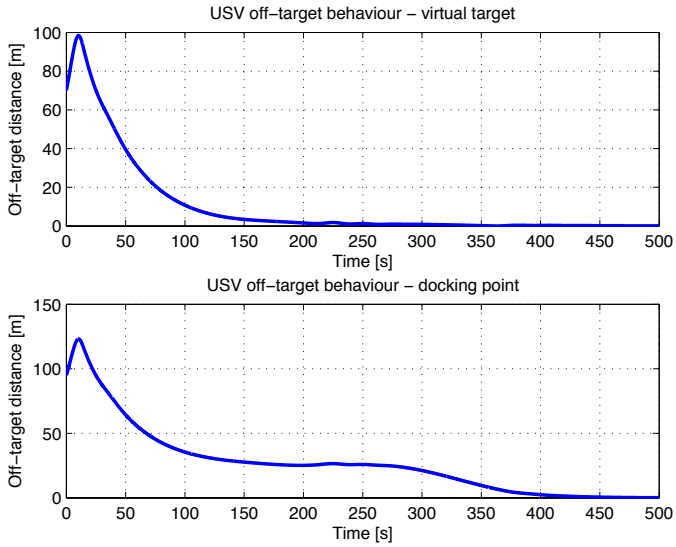

Figure 7.12: Off-target behaviour for the USV's position $\mathbf{p}_{\text{USV}}$, towards the virtual target $\mathbf{p}_{\text{t,USV}}$ and the docking station $\mathbf{p}_{\text{dock}}$.

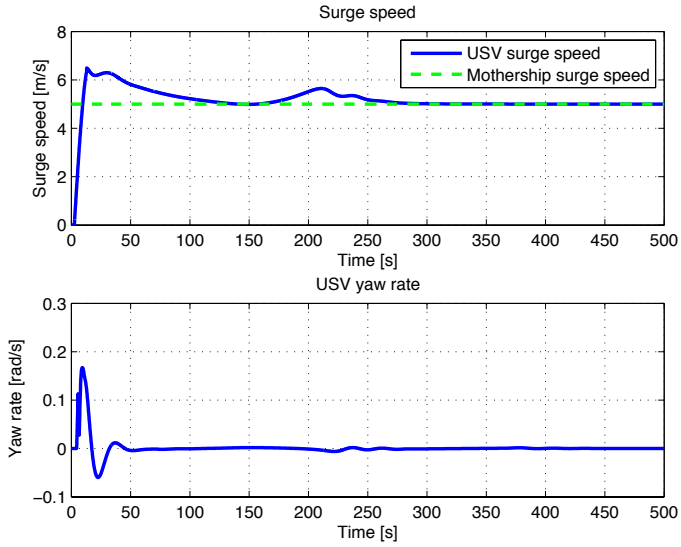

Figure 7.13: Surge speed and yaw rate, with mothership speed chosen to $5\,m/s$.

Curved mothership path

To illustrate that the mothership does not have to follow an exactly straight path, a constant rotation rate is applied to the mothership. The rotation rate is set to $0.001\,rad/s$, which makes the mothership turn slowly towards starboard side. To compensate for the increase in sideway motion the maximum approach speed towards the mothership is lowered to $\mathrm{U}_{\mathrm{t,max}} = 0.2\,m/s$. Besides from the newly introduced rotation rate and the reduction in maximum approach speed, the parameters are the same as in the first case where the mothership had a forward speed of $3\,m/s$.

In Figure 7.14 a NED-frame plot relative to the mothership is shown, where it can be observed that the USV approaches the mothership in same manners as during the first straight path case. To observe the real difference, the whole docking procedure is given in a standard NED-frame plot in Figure 7.15. Here it can be observed that the mothership slowly turns towards starboard and that the USV then follows with the same turn to complete docking. The final docking segment is showed in Figure 7.16, where it can be observed that the USV converges nicely towards the mothership regardless of the mothership's steering.

Finally in Figure 7.17 and Figure 7.18 it can be seen that the off-target behaviour and the velocity assignments are satisfying and does not deviate much from the original straight path case. This feature which allows the USV to dock with a turning mothership is nice to have in a boundary restricted sea where the shore or other vessels prevents the mothership to travel on a straight course.

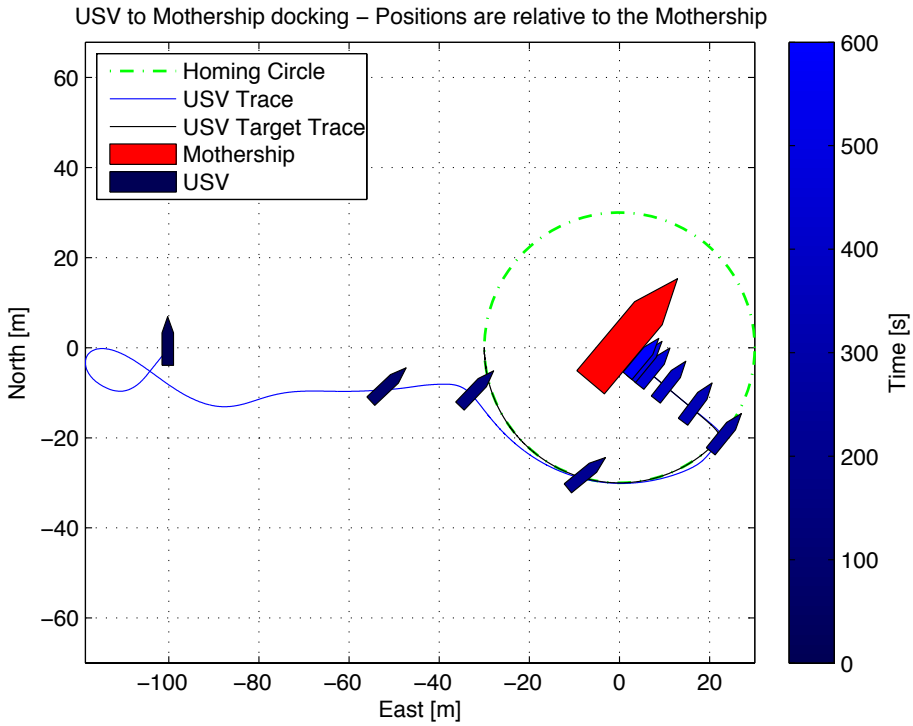

Figure 7.14: The USV closing upon the mothership which traverses with a curved path and manoeuvres into docking position. Coordinates are given relative to the mothership, where the north and east direction are according to the initial orientation of the mothership.

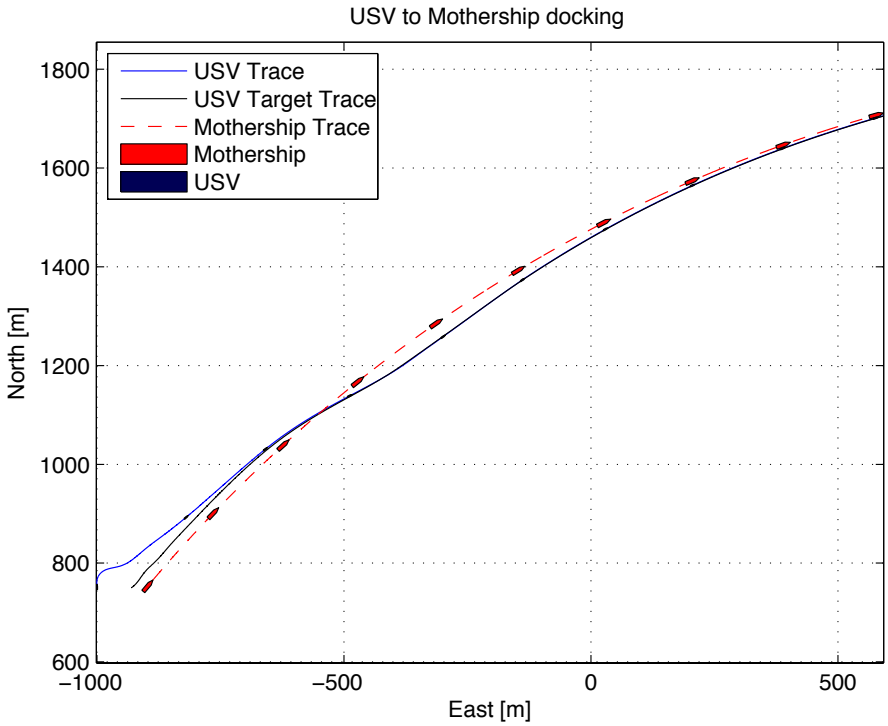

Figure 7.15: The USV closing up and then finalise docking with the mothership which travels a curved path.

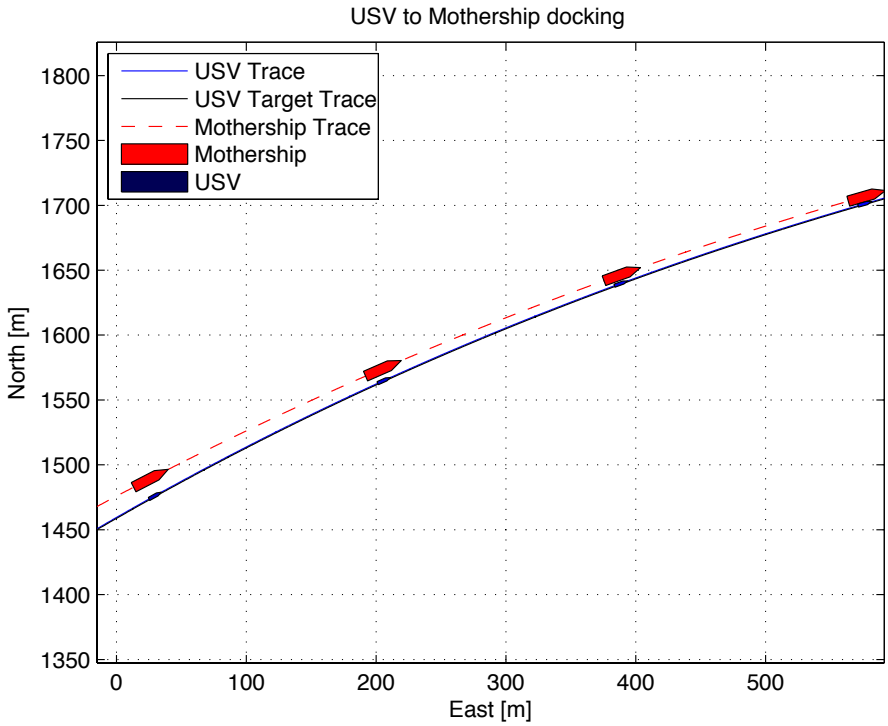

Figure 7.16: The final segment of the USV to mothership docking to shown to indicate the USV's approach during a curved mothership path.

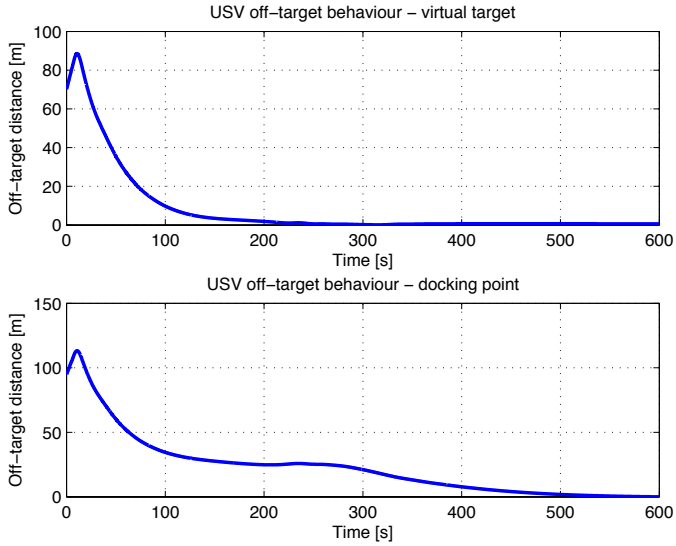

Figure 7.17: Off-target behaviour for the USV's position $\mathbf{p}_{\mathrm{USV}}$, towards the virtual target $\mathbf{p}_{\mathrm{t,USV}}$ and the docking station $\mathbf{p}_{\mathrm{dock}}$ during the curved path case.

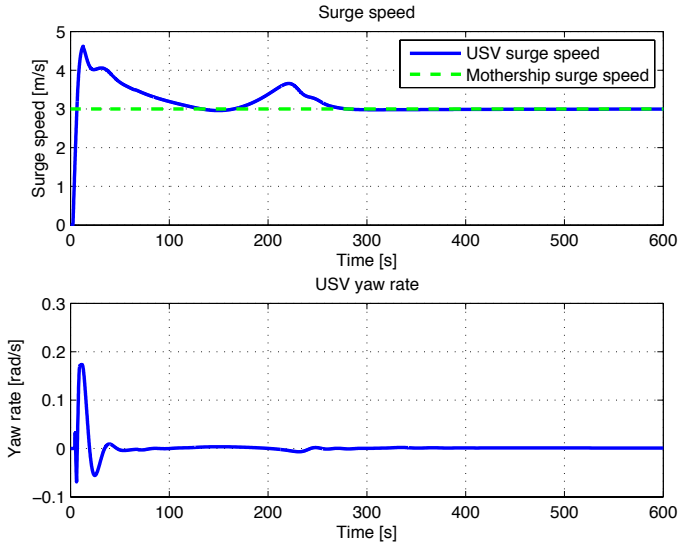

Figure 7.18: Surge speed and yaw rate for the curved path case.

Chapter 8

Conclusions and Future Work

This master thesis has shown two independent marine docking scenarios which includes the docking of an AUV together with a USV, and the docking of a USV with a manned mothership without human interference. The guidance laws developed shows an interesting approach of the docking vehicles. Since the vehicles are assumed underactuated, and in this case only has controllability over surge speed and yaw rate, a rendezvous docking strategy is chosen, where both vehicles are in motion during final docking. This is especially exploited during the USV to mothership scenario where the USV has to dock sideways into the mothership and therefore has to take advantage of the motherships forward motion to converge sideways. Here it is shown throughout simulations that how fast the USV can move sideways without slanting towards the mothership is strongly correlated with the mothership's speed, where higher speed equals faster convergence and vice versa.

The docking vehicle utilise a collision avoidance strategy during the docking procedure, where in the AUV to USV docking the USV chooses between three different paths, which all are aligned against the wind direction to avoid crucial sideslip motion. In the USV to mothership scenario the USV avoid collision by manoeuvre around a circle until it reaches a desirable position, from which it has a clear path towards the docking station located on the mothership. In the simulations carried out, it can be observed that the docking vehicles steers clear of any collisions, where in the AUV to USV docking it chooses a correct path and in the latter docking scenario the USV follows the circle around the mothership satisfactorily.

Rendezvous variables were developed to prevent an update of the target movement laws, and to prevent the target from converging towards the docking point without a proper tracking of its virtual target. This shows to be an interesting and satisfying element to achieve a controlled environment. Also the docking point which can be located in an arbitrary position relative to the USV or the mothership has a huge potential in the variety of methods. These two elements have been developed such that the docking methods are robust and could be used on many general marine docking operations and vehicles, and not just the two scenarios showed here.

8.1 Future Work

As usual during scientific work, there remain loads of additional work. Here are some recommendations for future research and development:

- Include and explore the influence of different environmental disturbances and find the threshold where docking can not longer be performed.
- Develop a 6DOF robust control model specialised for the docking scenario.
- Optimise the docking methods regarding to consumed time and area.
- Find practical aspects such as suitable docking stations for both scenarios.
- Optimise algorithms regarding to simulation time and real-time standards to perform sea trials.
- Combine several vessels which in the end will lead to a complete fleet of AUVs and USVs working together, and where the AUV or USV has to find the closest available vessel to dock with.

Bibliography

Breivik, M. & Fossen, T. I. (2009). Guidance Laws for Autonomous Underwater Vehicles. In *A. V. Inzartsev (Ed.), "Underwater Vehicles"* (pp. 51–76). INTECH Education and Publishing.

Breivik, M., Hovstein, V. E., & Fossen, T. I. (2008). Straight-Line Target Tracking for Unmanned Surface Vehicles. *Modeling, Identification and Control, 29*(4), 131–149.

Department of Defense (2002). Joint doctrine and joint tactics, techniques, and procedures for air mobility operations. In *Joint Publication 3-17. Washington, USA.*

Dunbabin, M., Lang, B., & Wood, B. (2008). Vision-based docking using an autonomous surface vehicle. In *Proceedings of the IEEE International Conference on Robotics and Automation. Pasadena, CA, USA.*

Fehse, W. (2003). *Automated Rendezvous and Docking of Spacecraft.* Cambridge University Press, Cambridge, United Kingdom.

Fossen, T. I. (2002). *Marine Control Systems: Guidance, Navigation and Control of Ships, Rigs and Underwater Vehicles.* Marine Cybernetics, Trondheim, Norway.

Hong, Y. H., Kim, J. Y., Lee, P. M., Jeon, B. H., Oh, K. H., & Oh, J. (2003). Development of the homing and docking algorithm for AUVs. In *Proceedings of the 13th International Offshore and Polar Engineering Conference. Honolulu, Hawaii, USA.*

Jantapremjit, P. & Wilson, P. A. (2008). Guidance-control based path following for homing and docking using an autonomous underwater vehicle. In *OCEANS 2008-MTS/IEEE Techno-Ocean. Kobe, Japan.*

Khalil, H. (2002). *Nonlinear systems.* Upper Saddle River, NJ: Prentice Hall.

Kongsberg Maritime (2010). Homepage: `http://www.km.kongsberg.com/`. [Online; accessed May-21-2010].

Martins, A., Almeida, J. M., Ferreira, H., Silva, H., Dias, N., Dias, A., Almeida, C., & Silva, E. P. (2007). Autonomous surface vehicle docking manoeuvre with visual information. In *Proceedings of the 2007 IEEE International Conference on Robotics and Automation. Roma, Italy.*

Perez, T. (2005). *Ship Motion Control.* Springer, London, UK.

Rae, G. J. S. & Smith, S. M. (1992). A fuzzy rule based docking procedure for autonomous underwater vehicles. In *Proceedings of the OCEANS'92. Newport, Rhode Island, USA.*

SNAME (1950). The Society of Naval Architects and Marine Engineers. Nomenclature of Treating the Motion of a Submerged Body. *Technical and Research Bulletin No. 1-5.*

Spong, M. W., Hutchinson, S., & Vidyasagar, M. (2006). *Robot Modeling and Control.* Wiley, New Jersey, USA.

The Department for Business, Innovation and Skills (BIS) (2010). Homepage: `http://www.bis.gov.uk/`. [Online; accessed May-27-2010].

Wertz, J. R. & Bell, R. (2003). Autonomous rendezvous and docking technologies - Status and prospects. In *Proceedings of the Space Systems Technology and Operations Conference. Orlando, Florida.*

Yakimenko, O. A., Horner, D. P., & Pratt, D. G. (2008). AUV rendezvous trajectories generation for underwater recovery. In *Proceedings of the 16th Mediterranean Conference on Control and Automation. Ajaccio France.*

Appendix A

CD contents

Articles - Folder

Filename:	*Description:*
Breivik 2008.pdf	Breivik et al. (2008)
Breivik 2009.pdf	Breivik & Fossen (2009)
DoF 2002.pdf	Department of Defense (2002)
Dunbabin 2008.pdf	Dunbabin et al. (2008)
Hong 2003.pdf	Hong et al. (2003)
Jantapremjit 2008.pdf	Jantapremjit & Wilson (2008)
Martins 2007.pdf	Martins et al. (2007)
Rae 1992.pdf	Rae & Smith (1992)
Sname 1950.pdf	SNAME (1950)
Wertz 2003.pdf	Wertz & Bell (2003)
Yakimenko 2008.pdf	Yakimenko et al. (2008)

Matlab code/AUV docking - Folder

Filename:	*Description:*
mariner	Mariner USV model
viknes	Viknes USV model
angle_mapping.m	Mapping angles $[-\pi\,,\,\pi]$ to $[0\,,\,2\pi]$
AUV_docking.mdl	Simulink diagram
chi_tilde.m	Function for calculation $\tilde{\chi}(t)$
circle.m	Circle plotting function
Initialisation.m	Initialisation file
myPlot.m	Matlab file for plotting results
usv_virutal_target.m	Calculates the USV's virtual target

Matlab code/USV docking - Folder

Filename:	*Description:*
viknes	Viknes USV model
angle_mapping.m	Mapping angles $[-\pi\,,\,\pi]$ to $[0\,,\,2\pi]$
cbhandle.m	Used by cblabel.m
cblabel.m	Allowing to labelling colorbars
chi_tilde.m	Function for calculation $\tilde{\chi}(t)$
circle.m	Circle plotting function
Initialisation.m	Initialisation file
myPlot.m	Matlab file for plotting results
USV_docking.mdl	Simulink diagram

Report.pdf - File